UNITED NATIONS EDUCATIONAL, SCIENTIFIC AND CULTURAL ORGANIZATION
INTERNATIONAL ATOMIC ENERGY AGENCY
INTERNATIONAL CENTRE FOR THEORETICAL PHYSICS
I.C.T.P., P.O. BOX 586, 34100 TRIESTE, ITALY, CABLE: CENTRATOM TRIESTE

H4.SMR/1058-3

WINTER COLLEGE ON OPTICS

9 - 27 February 1998

Fundamentals of Nonlinear Optics

M. Kauranen

**Research Centre on Molecular Electronics and Photonics,
University of Leuven, Belgium**

ICTP/ICO Winter College on Optics 1998

Trieste, Italy, February 9-27, 1998

FUNDAMENTALS OF NONLINEAR OPTICS

Martti Kauranen
Laboratory of Chemical and Biological Dynamics and
Research Center on Molecular Electronics and Photonics,
University of Leuven, Belgium

Contents

1. Introduction

These lectures provide an introduction to the fundamental concepts of nonlinear optics. The field of nonlinear optics is too large to be covered in a comprehensive way in the limited amount of time available. Hence, we will spend most of the time on discussing the basic formalism of nonlinear optics and effects that could be said to represent the most traditional nonlinear optical processes. The remaining time will be devoted to topics that are related to the development and characterization of organic nonlinear optical materials.

Common to the topics covered is that they can be described using the nonlinear susceptibility (or hyperpolarizability) formalism. For example, in the electric-dipole approximation, the material response (polarization) to the optical field is expanded in power series of the applied electric field as

$$P = \chi^{(1)}E + \chi^{(2)}E^2 + \chi^{(3)}E^3 + \ldots \tag{1.1}$$

The quantities χ represent material susceptibilities of different orders and form the basis for traditional nonlinear optics.

The power expansion (1.1) is not always valid. For example, when the optical field is strongly resonant with the material, the effective susceptibility is sometimes of the form

$$\chi = \frac{\chi_0}{1 + I/I_s}\ , \tag{1.2}$$

where I is the intensity of the optical field and I_s is a quantity characteristic to the material known as saturation intensity. It is clear that when the field intensity exceeds the saturation intensity, the power expansion of the type of Eq. (1.1) does not converge. Such saturation effects are not covered in these lectures. Other important topics not covered are: stimulated scattering processes (e.g., Brillouin, Raman, and Rayleigh scattering), acousto-optic effects, and photorefractive effects.

The lectures are based on the Gaussian system of units. The reason for this is that several textbooks in the field are written in Gaussian units. In addition, a large number of scientific publications still use these units.

Notationally, the lectures follow closely the textbook of Boyd [1]. This book is quite accessible to a researcher entering the field of nonlinear optics. Nevertheless, it also covers topics that are quite advanced. Another general textbook in the field is the book of Shen [2], which is on a more advanced level than Boyd. In addition, the book of Butcher and Cotter [3] provides a more mathematical and theoretically oriented approach to nonlinear optics. The books of Prasad and Williams [4] and Bosshard *et al.* [5] cover the field of organic nonlinear optics. References [6-11] are other books related to the general topic of the lectures.

2. Nonlinear Optics

2.1 Origin of nonlinear response

We begin by noting that the response of any system to an external perturbation will become nonlinear when the perturbation is strong enough. For example, when a spring is stretched (Fig. 2.1), the displacement x and applied force F are related by

$$F = k_1 x + k_2 x^2 + \ldots \tag{2.1}$$

When the force is small, only the term $k_1 x$ is important. However, it is clear that when the force is sufficiently increased, the displacement can not be increased in the same proportion. Hence, we can expect that the higher-order terms become important when the displacement is large.

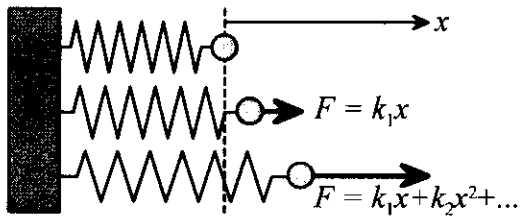

Figure 2.1. Nonlinear response of a spring to an applied force

A model of the type of Fig. 2.1 with an electron attached to the end of a spring can be used to predict nonlinear optical properties from a purely classical model (see, e.g., [1]).

2.2 Nonlinear optical susceptibility

In nonlinear optics, we are interested in effects where the response of a material to the optical field becomes nonlinear. Most materials respond strongest to the electric component of the electromagnetic field. This response will polarize the material. The polarization will then act as a source of new radiation.

The polarization can often be expanded in power series in the applied field as

$$\mathbf{P}(t) = \chi^{(1)} \cdot \mathbf{E}(t) + \chi^{(2)} : \mathbf{E}^2(t) + \chi^{(3)} : \mathbf{E}^3(t) + \ldots \tag{2.2}$$

Here $\chi^{(1)}$ is the linear susceptibility tensor that gives rise to linear refractive index and linear absorption. $\chi^{(2)}$ and $\chi^{(3)}$ are the second- and third-order nonlinear susceptibility tensors, respectively, and so on. Most important nonlinear effects are second- and third-order processes.

2.3 Complex notation

We will use complex notation for the fields and polarizations. Each frequency component of the field is expressed as

$$\mathbf{E}(t) = \mathbf{E}(\omega) e^{-i\omega t} + \mathbf{E}^*(\omega) e^{i\omega t}. \tag{2.3}$$

The field amplitude $\mathbf{E}(\omega)$ at frequency ω can contain any number of beams propagating to different spatial directions characterized by different wave vectors.

2.4 Examples of nonlinear effects

By inserting Eq. (2.3) into Eq. (2.2), we find that the second-order response contains a polarization component

$$\mathbf{P}^{(2)}(t) = \chi^{(2)} : \mathbf{E}^2(\omega) e^{-i2\omega t}, \tag{2.4}$$

that oscillates at twice the fundamental frequency. Hence, we conclude that nonlinear processes can generate radiation at new frequencies (Fig. 2.2). Such frequency conversion is one of the most important applications of nonlinear optics.

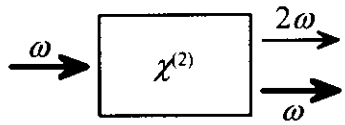

Figure 2.2. Frequency doubling in a second-order material.

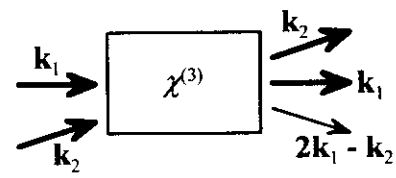

Figure 2.3. Generation of a new beam through third-order nonlinearity.

It is easy to show that the third-order response contains a term of the form

$$\mathbf{P}^{(3)}(t) = 3\chi^{(3)} : \mathbf{E}(\omega)\mathbf{E}(\omega)\mathbf{E}^*(\omega) e^{-i\omega t}. \tag{2.5}$$

For the case of two beams propagating in different directions, we have

$$\mathbf{E}(\omega) = \mathbf{A}_1 e^{i\mathbf{k}_1 \cdot \mathbf{r}} + \mathbf{A}_2 e^{i\mathbf{k}_2 \cdot \mathbf{r}}, \tag{2.6}$$

and the nonlinear polarization contains the following term

$$\mathbf{P}^{(3)}(\omega) = 3\chi^{(3)} : \mathbf{A}_1^2 \mathbf{A}_2^* e^{i(2\mathbf{k}_1 - \mathbf{k}_2)\cdot \mathbf{r}}. \tag{2.7}$$

The spatial dependence of this term suggests that nonlinear processes can generate beams that propagate in different directions than the applied beams (Fig. 2.3).

In general, we can define nonlinear optics as the field that studies effects that occur when the optical properties of a material are modified by the very presence of light.

3. Nonlinear Optical Susceptibility

3.1 Definition of nonlinear optical susceptibility

We assume that the optical field can be expressed as a sum over contributions at several discrete frequencies as

$$\mathbf{E}(t) = \sum_n \left[\mathbf{E}(\omega_n)e^{-i\omega_n t} + \mathbf{E}^*(\omega_n)e^{i\omega_n t}\right], \tag{3.1}$$

where the summation is over positive frequencies. By extending the summation to include also the negative frequencies, this can be expressed as

$$\mathbf{E}(t) = \sum_n \mathbf{E}(\omega_n)e^{-i\omega_n t} . \tag{3.2}$$

The reality of the total field requires that the amplitudes of the negative and positive frequency parts are related by

$$\mathbf{E}(-\omega_n) = \mathbf{E}^*(\omega_n) . \tag{3.3}$$

Analogous to Eq. (3.2), we also expand the material polarization as a sum over different frequency components as

$$\mathbf{P}(t) = \sum_n \mathbf{P}(\omega_n)e^{-i\omega_n t} . \tag{3.4}$$

The electric field and polarization are vectorial quantities. In addition, the susceptibilities are expected to depend on the frequencies of the optical field. We therefore define the second-order susceptibility tensor formally as [1]

$$P_i(\omega_p + \omega_q) = \sum_{jk} \sum_{(pq)} \chi^{(2)}_{ijk}(\omega_p + \omega_q; \omega_p, \omega_q) E_j(\omega_p) E_k(\omega_q) , \tag{3.5}$$

where the indices *ijk* refer to the Cartesian coordinates and the notation *(pq)* indicates that $\omega_p + \omega_q$ is to be held fixed in summation over p and q.

The summation over p and q can be explicitly performed. In the presence of two different frequencies ω_p and ω_q, we obtain

$$P_i(\omega_p + \omega_q) = \sum_{jk} 2\chi^{(2)}_{ijk}(\omega_p + \omega_q; \omega_p, \omega_q) E_j(\omega_p) E_k(\omega_q) , \tag{3.6}$$

where the intrinsic permutation symmetry

$$\chi^{(2)}_{ikj}(\omega_p + \omega_q; \omega_q, \omega_p) = \chi^{(2)}_{ijk}(\omega_p + \omega_q; \omega_p, \omega_q) , \tag{3.7}$$

was used. For the case of one input frequency, we obtain

$$P_i(2\omega_p) = \sum_{jk} \chi^{(2)}_{ijk}(2\omega_p;\omega_p,\omega_p)E_j(\omega_p)E_k(\omega_p). \tag{3.8}$$

We note that the susceptibilities are sometimes defined in such a way that the numerical factors [e.g., 2 in Eq. (3.6)] arising from summation over p and q are absorbed into the susceptibility.

The third-order susceptibility is defined in a way analogous to Eq. (3.5) as

$$P_i(\omega_p+\omega_q+\omega_r) = \sum_{jkl}\sum_{(pqr)} \chi^{(2)}_{ijkl}(\omega_p+\omega_q+\omega_r;\omega_p,\omega_q,\omega_r)E_j(\omega_p)E_k(\omega_q)E_l(\omega_r). \tag{3.9}$$

The second-order susceptibility is a third-rank tensor. Hence, it has in general $3^3 = 27$ independent complex-valued components. Similarly, the third-order susceptibility has $3^4 = 81$ independent components. The number of independent components can fortunately be reduced by symmetry arguments.

3.2 Photon diagrams

The nonlinear response can be understood in terms of photon diagrams as shown in Fig. 3.1. For example, the interaction

$$\chi^{(2)}(\omega_p+\omega_q;\omega_p,\omega_q)E(\omega_p)E(\omega_q), \tag{3.10}$$

indicates that the photons at the positive input frequencies ω_p and ω_q excite the material to virtual states (upward thick arrows) and are annihilated. A photon at the frequency $\omega_p+\omega_q$ is simultaneously created (downward thin arrow).

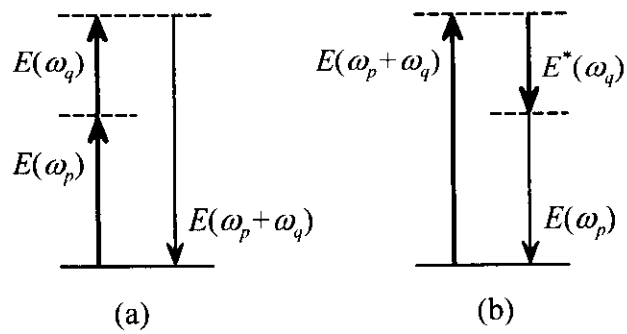

Figure 3.1. Photon diagrams for sum- (a) and difference- (b) frequency generation.

The other example is difference frequency generation

$$\chi^{(2)}(\omega_p;\omega_p+\omega_q,-\omega_q)E(\omega_p+\omega_q)E(-\omega_q)$$
$$= \chi^{(2)}(\omega_p;\omega_p+\omega_q,-\omega_q)E(\omega_p+\omega_q)E^*(\omega_q). \tag{3.11}$$

Here we apply the rule that the field at the negative frequency (i.e., the conjugate part of the field) drives the system down in energy. At the same time, a photon at this frequency is also created.

3.3 Microscopic vs. macroscopic response

We have defined the susceptibility for a macroscopic material in the laboratory frame of reference. However, the macroscopic response is due to the microscopic response of the building units of the material. For the case of crystals, the building units are the unit cells of the crystalline lattice. For the case of molecular (or atomic) media, the response originates from the individual molecules.

For molecules of low symmetry, the molecules themselves have a preferred coordinate system. Analogous to Eq. (2.2), the microscopic molecular dipole moment is expressed as

$$\mu = \mu_0 + \alpha \cdot \mathbf{E} + \beta : \mathbf{E}^2 + \gamma \vdots \mathbf{E}^3 + \ldots \tag{3.12}$$

where μ_0 is the permanent dipole moment of the molecules, α is the linear polarizability, and β and γ are the first and second hyperpolarizability tensors, respectively.

For the case of second-order quantities, the relation between the molecular and macroscopic quantities is (Fig. 3.2)

$$\chi^{(2)}_{ijk} = N\left\langle f(\omega_p + \omega_q) f(\omega_p) f(\omega_q) \beta_{IJK} \cos(i,I)\cos(j,J)\cos(k,K)\right\rangle, \tag{3.13}$$

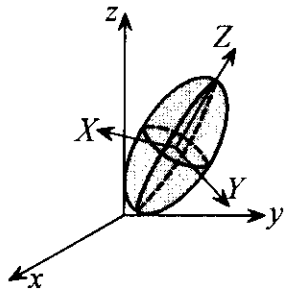

Figure 3.2. Transformation between the molecular (*XYZ*) and laboratory (*xyz*) frames of reference.

where the upper- and lower-case subscripts refer to the molecular and macroscopic frames of reference, respectively, the brackets denote averaging over the orientational distribution of the molecules, N is the number density of the molecules, and f are the local-field factors.

The local-field factors account for the difference between the macroscopic and microscopic fields. The individual molecules respond to the local field, which includes the applied external field and the field due to the surrounding molecules, whereas the susceptibilities are defined in terms of the macroscopic field. No general way of accounting for the local fields exists. However, the local-field factors are usually approximated by

$$f(\omega) = \frac{\varepsilon(\omega) + 2}{3}, \tag{3.14}$$

where $\varepsilon(\omega)$ is the linear dielectric constant. By appropriately combining materials of low and

high dielectric constants, the local field effects can be used to enhance the nonlinear response [12-14].

3.4 Quantum-mechanical result

For the case of electronic nonlinearities, expressions for the molecular polarizabilities can be derived from quantum mechanics. Two different approaches can be taken. The first is based on a Schrodinger equation (wavefunction) calculation and leads to results that are valid when the optical frequencies are detuned far from the resonance frequencies of the material. However, close to material resonances, dissipative processes (damping of the material response) become important. Such damping effects are better treated using the density matrix formalism [1,15].

When all molecules are assumed to be initially in their ground state, a density matrix calculation yields the first hyperpolarizability (second-order response) in the form

$$\begin{aligned}\beta_{IJK}(\omega_p+\omega_q;\omega_p,\omega_q)=\frac{1}{2\hbar^2}\sum_{mn}\Bigg[&\frac{\mu_{gn}^I\mu_{nm}^J\mu_{mg}^K}{(\omega_{ng}-\omega_p-\omega_q-i\gamma_{ng})(\omega_{mg}-\omega_p-i\gamma_{mg})}\\&+\frac{\mu_{gn}^I\mu_{nm}^K\mu_{mg}^J}{(\omega_{ng}-\omega_p-\omega_q-i\gamma_{ng})(\omega_{mg}-\omega_q-i\gamma_{mg})}\\&+\left[1+\frac{i(\gamma_{mn}-\gamma_{ng}-\gamma_{mg})}{\omega_{mn}-\omega_p-\omega_q-i\gamma_{mn}}\right]\frac{\mu_{gn}^K\mu_{nm}^I\mu_{mg}^J}{(\omega_{ng}+\omega_p+i\gamma_{ng})(\omega_{mg}-\omega_q-i\gamma_{mg})}\\&+\left[1+\frac{i(\gamma_{mn}-\gamma_{ng}-\gamma_{mg})}{\omega_{mn}-\omega_p-\omega_q-i\gamma_{mn}}\right]\frac{\mu_{gn}^J\mu_{nm}^I\mu_{mg}^K}{(\omega_{ng}+\omega_q+i\gamma_{ng})(\omega_{mg}-\omega_p-i\gamma_{mg})}\\&+\frac{\mu_{gn}^K\mu_{nm}^J\mu_{mg}^I}{(\omega_{mg}+\omega_p+\omega_q+i\gamma_{mg})(\omega_{ng}+\omega_p+i\gamma_{ng})}\\&+\frac{\mu_{gn}^J\mu_{nm}^K\mu_{mg}^I}{(\omega_{mg}+\omega_p+\omega_q+i\gamma_{mg})(\omega_{ng}+\omega_q+i\gamma_{ng})}\Bigg].\end{aligned}\tag{3.15}$$

where g is the ground state of the molecules, m and n refer to the excited states, μ_{nm} is the dipole transition moment, $\hbar\omega_{nm}=E_n-E_m$ the energy difference, and γ_{nm} the damping rate between states n and m. The wavefunction result is obtained by setting all damping rates to zero in Eq. (3.15).

The damping rates (linewidths) γ_{nm} of the transitions are small compared to the resonance frequencies ω_{nm}. Eq. (3.15) shows that the nonlinear

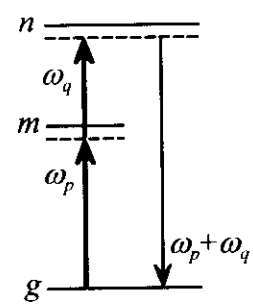

Figure 3.3. Resonance enhancement of susceptibility.

response can be greatly enhanced by tuning any of the frequencies ω_p, ω_q, or $\omega_p + \omega_q$ close to the resonance frequencies of the material (Fig. 3.3). The drawback of this strategy is that such resonances can often lead to losses because of linear absorption associated with the resonance.

3.5 Symmetry principles

The number of independent components of the susceptibility and hyperpolarizability tensors can be greatly reduced by symmetry principles.

Because the total optical field and polarization are real quantities, we have

$$\mathbf{E}(-\omega_n) = \mathbf{E}^*(\omega_n) \text{ and } \mathbf{P}(-\omega_n) = \mathbf{P}^*(\omega_n). \tag{3.16}$$

Consequently, the nonlinear tensors satisfy the symmetry property

$$\chi^{(2)}_{ijk}(-\omega_p - \omega_q; -\omega_p, -\omega_q) = \chi^{(2)}_{ijk}(\omega_p + \omega_q; \omega_p, \omega_q)^*. \tag{3.17}$$

The intrinsic permutation symmetry is

$$\chi^{(2)}_{ikj}(\omega_p + \omega_q; \omega_q, \omega_p) = \chi^{(2)}_{ijk}(\omega_p + \omega_q; \omega_p, \omega_q) \tag{3.18}$$

and was already used in Eqs. (3.6) and (3.7). There is no fundamental reason for this symmetry. However, it is useful for book keeping in Eqs. (3.5) and (3.9) and the susceptibility is usually defined so that this symmetry is fulfilled. This symmetry implies that the frequencies ω_p and ω_q can be freely interchanged as long as the indices j and k are simultaneously interchanged.

The nonlinear material can be assumed to be lossless when the optical frequencies are detuned far from the material resonances. The damping rates γ can then be neglected in Eq. (3.15). Consequently, the susceptibility (or hyperpolarizability) is a real quantity for lossless media. In the same limit, the susceptibility can be shown to satisfy the full permutation symmetry, which implies that all frequencies can be freely permuted as long as the indices i, j, and k are simultaneously permuted. In applying this rule, we have to remember that the output frequency is always the sum of the two input frequencies. For example

$$\chi^{(2)}_{ijk}(\omega_p + \omega_q; \omega_p, \omega_q) = \chi^{(2)}_{jki}(-\omega_p; \omega_q, -\omega_p - \omega_q). \tag{3.19}$$

The optical frequencies are often much smaller than any of the resonance frequencies of the material. The susceptibility can then be assumed to be independent of the frequencies. In this case, the indices i, j, and k can be permuted without permuting the frequencies, i.e.,

$$\chi^{(2)}_{ijk} = \chi^{(2)}_{ikj} = \chi^{(2)}_{jki} = \chi^{(2)}_{jik} = \chi^{(2)}_{kij} = \chi^{(2)}_{kji}. \tag{3.20}$$

This symmetry is known as Kleinman symmetry and it can greatly simplify the description of nonlinear optical interactions. However, one must be very careful in justifying it in practical situations.

3.6 Spatial symmetry

The nonlinear susceptibility (and hyperpolarizability) tensors must also satisfy conditions that reflect the spatial point-group symmetry [16,17] of the material. Probably the most powerful symmetry rule is the requirement of noncentrosymmetry for second-order (and other even-order) processes.

Centrosymmetric materials have spatial inversion as a symmetry operation. This operation implies that the material looks the same when the sign of each spatial coordinate is inverted, i.e.,

$$\mathbf{r} \rightarrow -\mathbf{r}\,. \tag{3.21}$$

The electric field and polarization transform similar to the position vector $\mathbf{r}$ [18]. Consequently,

$$-\mathbf{P}^{(2)} = \chi^{(2)} : (-\mathbf{E})^2 = \chi^{(2)} : \mathbf{E}^2 = \mathbf{P}^{(2)} = 0\,. \tag{3.22}$$

The second-order susceptibility tensor must therefore vanish in all centrosymmetric materials. This is a very powerful rule because 11 of the 32 point groups of crystals are centrosymmetric.

In addition, the nonlinear tensors must be compatible with any other spatial symmetry operations of the material.

The symmetry requirements are equally applicable on microscopic and macroscopic levels. Therefore, for second-order nonlinear optics one needs molecules (or other building units) with a noncentrosymmetric microscopic structure. In addition, such molecules must be organized in a macroscopically noncentrosymmetric way.

4. Wave-Equation Description

4.1 Wave equation

Starting from Maxwell's equations for the electromagnetic field, one can derive the wave equation for the propagating optical field. For transverse plane waves, the wave equation is

$$\nabla^2\mathbf{E} - \frac{1}{c^2}\frac{\partial^2\mathbf{E}}{\partial t^2} = \frac{4\pi}{c^2}\frac{\partial^2\mathbf{P}}{\partial t^2}. \tag{4.1}$$

where c is the speed of light and the polarization $\mathbf{P}$ contains both linear and nonlinear sources. This form can be used in most practical situations.

By considering a field component at frequency ω, the wave equation becomes

$$\nabla^2\mathbf{E}(\omega) + \frac{\omega^2}{c^2}\mathbf{E}(\omega) = -\frac{4\pi\omega^2}{c^2}\mathbf{P}(\omega). \tag{4.2}$$

We first consider linear propagation. The linear polarization is

$$\mathbf{P}(\omega) = \chi^{(1)} \cdot \mathbf{E}(\omega), \tag{4.3}$$

and the wave equation can be written as

$$\nabla^2\mathbf{E}(\omega) + \frac{\omega^2}{c^2}\left[1 + 4\pi\chi^{(1)}\right] \cdot \mathbf{E}(\omega) = 0. \tag{4.4}$$

We seek solutions in the form of plane waves propagating in the positive z direction and consider one of the eigenpolarizations of the material. The scalar amplitude of the eigenpolarization j is assumed to have the spatial dependence

$$E_j(\omega) = A_j e^{ik_j z}. \tag{4.5}$$

By inserting Eq. (4.5) into Eq. (4.4), we find that the wave vector is given by

$$k_j = n_j\omega / c, \tag{4.6}$$

where the linear index of refraction n_j is determined by

$$n_j^2 = 1 + 4\pi\chi_{jj}^{(1)}. \tag{4.7}$$

4.2 Spatial evolution of the nonlinear signal

We next consider the case where a nonlinear source $\mathbf{P}^{NL}(\omega)$ at frequency ω is also present. We again seek solution in the form of Eq. (4.5). However, due to the nonlinear interaction, we

allow the possibility that the amplitude A has spatial dependence. For a given polarization and using Eqs. (4.6) and (4.7), Eq. (4.2) can be manipulated into the form

$$\frac{d^2A(z)}{dz^2} + 2ik\frac{dA(z)}{dz} = -\frac{4\pi\omega^2}{c^2}P^{NL}(z)e^{-ikz}. \tag{4.8}$$

This can be further simplified by making the slowly-varying-amplitude approximation

$$\left|\frac{d^2A(z)}{dz^2}\right| << \left|k\frac{dA(z)}{dz}\right|. \tag{4.9}$$

This approximation implies that any significant variations in the amplitude A occur over several wavelengths. The spatial evolution of the slowly-varying amplitude is then found to be governed by the equation

$$\frac{dA(z)}{dz} = i\frac{2\pi\omega}{nc}P^{NL}(z)e^{-ikz}. \tag{4.10}$$

This is the fundamental equation to study spatial evolution of the nonlinear signal. The equation can be applied immediately once the form of the nonlinear source $P^{NL}(z)$ is known.

4.3 Phase matching

As an example of the application of Eq. (4.10), we consider frequency doubling from the fundamental frequency ω_1 to the second-harmonic frequency $\omega_2 = 2\omega_1$ (Fig 4.1). We assume that the fundamental beam also propagates in the positive z direction and is of the form

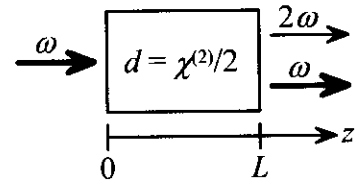

Figure 4.1. Second-harmonic generation.

$$E_1 = A_1e^{ik_1z}. \tag{4.11}$$

The nonlinear polarization at the second-harmonic frequency is then from Eq. (3.8)

$$P_2(z) = 2dA_1^2e^{i2k_1z}, \tag{4.12}$$

where $d = \chi^{(2)}/2$ and accounts for the tensor character of the interaction. We also assume that d is a real quantity. By inserting this into Eq. (4.10), we find the equation that governs the spatial evolution of the second-harmonic signal

$$\frac{dA_2}{dz} = i\frac{4\pi\omega_2}{n_2c}dA_1^2e^{i(2k_1-k_2)z} = i\frac{4\pi\omega_2}{n_2c}dA_1^2e^{i\Delta kz}. \tag{4.13}$$

Here the quantity

$$\Delta k = 2k_1 - k_2 \tag{4.14}$$

is known as the wave vector or phase mismatch between the fundamental and second-harmonic waves.

For now, we consider the case where only a small fraction of the fundamental intensity is converted into second-harmonic radiation so that A_1 can be taken as constant. We also assume the boundary condition $A_2(0) = 0$. For perfect phase matching $\Delta k = 0$, the solution of Eq. (4.13) is

$$A_2(L) = i\frac{4\pi\omega_2}{n_2 c} dA_1^2 L. \tag{4.15}$$

where L is the length of the nonlinear material.

The intensities of the fields are defined as

$$I = \frac{nc}{2\pi}|A|^2. \tag{4.16}$$

The intensity of the second-harmonic beam is then found to be

$$I_2(L) = \frac{32\pi^3\omega_2^2}{n_2 n_1^2 c^3}|d|^2 I_1^2 L^2. \tag{4.17}$$

The intensity grows quadratically as a function of the length of the nonlinear medium (Fig. 4.2).

For the case of $\Delta k \neq 0$, the solution is

$$A_2(L) = i\frac{4\pi\omega_2}{n_2 c} dA_1^2 \frac{e^{i\Delta kL} - 1}{i\Delta k} \tag{4.18}$$

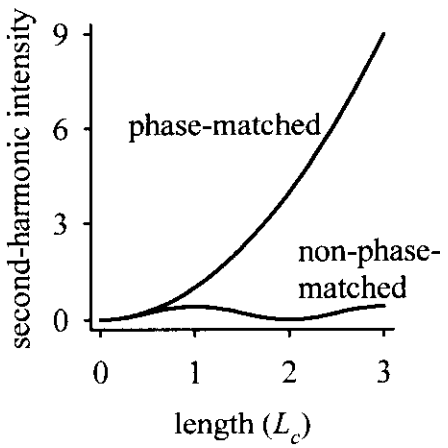

Figure 4.2. Growth of the second-harmonic intensity for phase-matched and non-phase-matched frequency doubling.

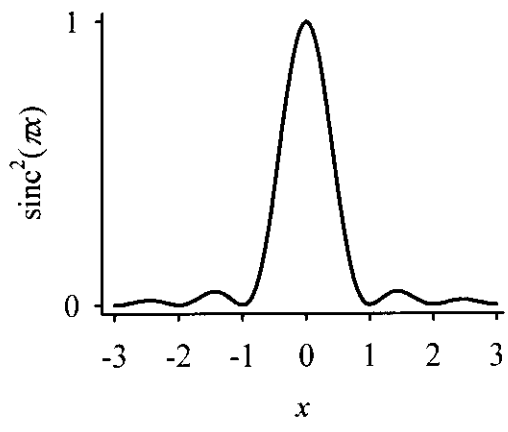

Figure 4.3. The sinc^2 function.

and the intensity is

$$I_2(L) = \frac{128\pi^3\omega_2^2}{n_2 n_1^2 c^3}|d|^2 I_1^2 \frac{\sin^2(\Delta kL/2)}{(\Delta k)^2} = \frac{32\pi^3\omega_2^2}{n_2 n_1^2 c^3}|d|^2 I_1^2 L^2 \mathrm{sinc}^2(\Delta kL/2). \quad (4.19)$$

For a given phase mismatch Δk, this solution oscillates sinusoidally as a function of the length of the medium (Fig. 4.2). The second-harmonic field reaches its first maximum at a distance

$$L_c = \pi/\Delta k, \quad (4.20)$$

into the medium. This distance is known as the coherence length. It is the maximum useful length that can be used for harmonic generation. Note that for $L = L_c$, the expressions (4.17) and (4.19) already differ by a factor of $\pi^2/4 \approx 2.5$.

The solution (4.19) is similar to that for the case of perfect phase matching [Eq. (4.17)] except for the factor

$$\mathrm{sinc}^2(\Delta kL/2). \quad (4.21)$$

This factor is plotted in Fig. 4.3. Phase matching is therefore seen to be one of the most important concepts in determining the efficiency of second-harmonic generation or any other frequency conversion process.

4.4 Interpretations of phase mismatch

In the previous section, the concept of phase mismatch arose in a somewhat abstract and mathematical way. However, it can be interpreted in various ways that are more physical. One interpretation is to note that a difference in $2k_1$ and k_2 signifies that the waves at the fundamental and second-harmonic fields propagate at different phase velocities in the material (Fig. 4.4). Consequently, the coherence length signifies a length after which the second-harmonic field and its driving polarization have ended up out of phase.

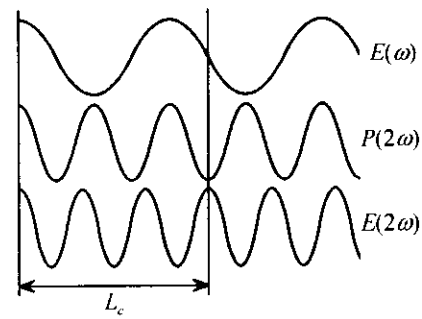

Figure 4.4. Second-harmonic field and its driving polarization end up out of phase after one coherence length.

Phase matching can also be interpreted as momentum conservation (Fig. 4.5). The linear momentum of a photon is $\hbar k$. Second-harmonic generation annihilates two photons from the fundamental beam and converts them into a single photon at

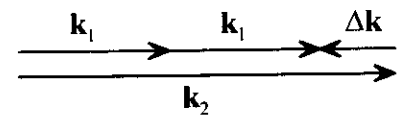

Figure 4.5. Phase matching as momentum conservation.

the second-harmonic beam. Therefore, conservation of linear momentum requires

$$2\hbar k_1 = \hbar k_2 . \tag{4.22}$$

which is equivalent to the phase-matching condition $\Delta k = 0$.

From the microscopic point of view, the nonlinear process sets the molecular dipoles oscillating at the second-harmonic frequency. Each dipole will then emit its characteristic dipole radiation pattern (Fig. 4.6). In the case of perfect phase matching, the phase relation of each oscillating dipole and the second-harmonic field is maintained. This leads to complete constructive interference in the forward direction. The intensity of N dipoles emitting in phase scales as N^2. The number of dipoles depends linearly on the length of the material and therefore explains the quadratic dependence on length L. This interpretation is analogous to the molecular theory of nonlinear optics, which accounts for the radiative properties of the elementary dipoles [19].

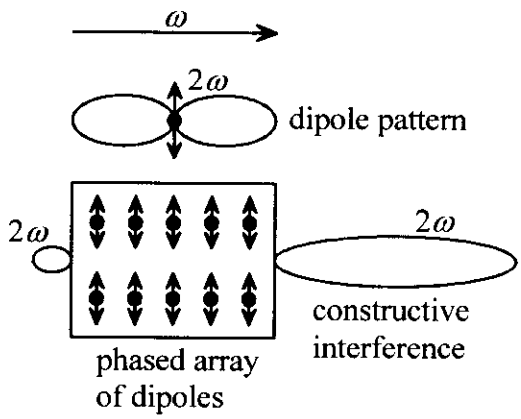

Figure 4.6. Molecular interpretation of phase matching.

4.5 Backward second-harmonic generation

The molecular interpretation of phase matching and Fig. 4.6 suggest that some second-harmonic light is also emitted in the backward direction. This is true and hence the assumption of the boundary condition $A_2(0) = 0$ is not strictly valid. However, the backward generated field is usually much weaker than the forward field, which validates the above treatment. It can be shown that the slowly-varying envelope approximation is equivalent to neglecting the backward generated second-harmonic field [2].

There are also situations where the forward and backward generated second-harmonic fields are approximately equally strong. This occurs when the length of the material is much smaller than the coherence length that phase matching considerations are unimportant. This is particularly the case for thin films and surfaces [2]. Several different formulations exist that properly account for the forward and backward generated fields in surface and thin-film nonlinear optics [2,20,21].

5. Second-Order Processes

5.1 Second-harmonic generation

In Section 4.3, we considered second-harmonic generation in the limit of an undepleted fundamental beam. This allowed us to introduce the fundamental concepts of frequency conversion processes. In most practical situations, however, one would like to convert as much as possible of the fundamental radiation into the second-harmonic radiation. The assumption of an undepleted fundamental beam is then clearly unjustified.

In the more general case, the nonlinear polarization at the second-harmonic frequency is

$$P_2(z) = 2dA_1^2(z)e^{i2k_1z}. \tag{5.1}$$

Note that we now allow $A_1(z)$ to be spatially varying. We must also consider the nonlinear polarization at the fundamental frequency due to the difference-frequency mixing ($\omega = 2\omega - \omega$) between the fundamental and second-harmonic beams. The nonlinear polarization describing this process is given by

$$P_1(z) = 4dA_2(z)A_1^*(z)e^{i(k_2-k_1)z} \tag{5.2}$$

In writing this equation, we have assumed that the nonlinear tensor possesses full permutation symmetry so that the nonlinear coefficient d is the same as in Eq. (5.1). These sources lead to the following equations governing the spatial evolution of the fields

$$\frac{dA_1}{dz} = i\frac{8\pi\omega_1}{n_1c}dA_2A_1^*e^{-i\Delta kz}, \tag{5.3}$$

$$\frac{dA_2}{dz} = i\frac{4\pi\omega_2}{n_2c}dA_1^2e^{i\Delta kz}. \tag{5.4}$$

The solutions to the coupled equations (5.3) and (5.4) are quite complicated [22]. For the case of perfect phase matching and no applied second-harmonic field they are

$$I_1(z) = \mathrm{sech}^2(z/z_0), \tag{5.5}$$

$$I_2(z) = \tanh^2(z/z_0), \tag{5.6}$$

where z_0 is a characteristic length. These results show that all fundamental radiation can be converted into second-harmonic radiation (Fig. 5.1). Of course, for this to occur, the nonlinear medium must be sufficiently long.

As expected, imperfect phase matching limits the maximum conversion efficiency. In this case, the energy flows back and forth between the fundamental and second-harmonic beams. Consequently, the net efficiency depends also on the exact length of the medium.

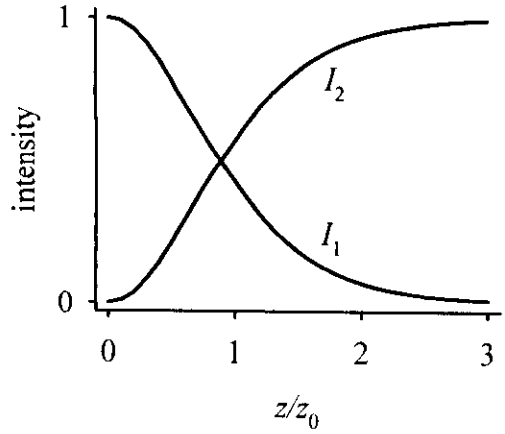

Figure 5.1. Evolution of fundamental and second-harmonic intensities in frequency doubling.

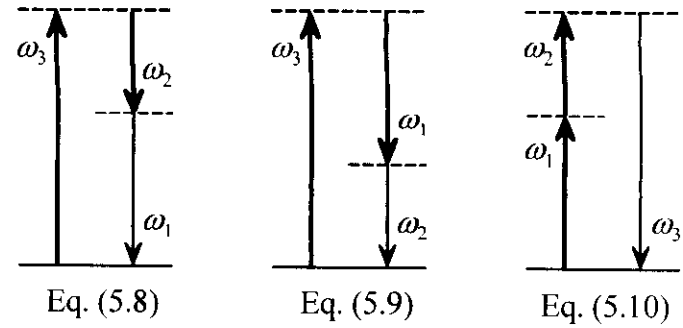

Figure 5.2. Photon diagrams for Eqs. (5.8)-(5.10). For Eq. (5.10), the ordering of the input photons can also be reversed.

5.2 Three-wave interactions

We next consider the general interaction between three waves at three different frequencies. For definiteness, we choose

$$\omega_3 = \omega_1 + \omega_2 . \tag{5.7}$$

Using the general techniques, we can derive the following three coupled-amplitude equations that describe the mutual evolution of the slowly-varying envelopes

$$\frac{dA_1}{dz} = i\frac{8\pi\omega_1}{n_1 c} dA_3 A_2^* e^{-i\Delta kz}, \tag{5.8}$$

$$\frac{dA_2}{dz} = i\frac{8\pi\omega_2}{n_2 c} dA_3 A_1^* e^{-i\Delta kz}, \tag{5.9}$$

$$\frac{dA_3}{dz} = i\frac{8\pi\omega_3}{n_3 c} dA_1 A_2 e^{i\Delta kz}, \tag{5.10}$$

where the phase mismatch is

$$\Delta k = k_1 + k_2 - k_3 . \tag{5.11}$$

Eq. (5.8) [(5.9)] describes generation of the field at frequency ω_1 (ω_2) through difference frequency generation between the frequencies ω_3 and ω_2 (ω_1). Eq. (5.10) describes sum-frequency generation of the field at frequency $\omega_3 = \omega_1 + \omega_2$. The photon diagrams of these processes are shown in Fig. 5.2.

5.3 Manley-Rowe relations

From Eqs. (5.8)-(5.10), we can derive the following equation that describes the total evolution of the intensities of the three waves

$$\frac{d}{dz}(I_1 + I_2 + I_3) = 0 . \tag{5.12}$$

This equation implies that the total intensity (energy) of the waves is conserved.

The number of photons in each beam is proportional to the quantity $I/\hbar\omega$. We can derive the following equation describing the evolution of the number of photons in each beam

$$\frac{1}{\omega_1}\frac{dI_1}{dz} = \frac{1}{\omega_2}\frac{dI_2}{dz} = -\frac{1}{\omega_3}\frac{dI_3}{dz} . \tag{5.13}$$

This result implies that the only possible processes are the ones where photons at frequencies ω_1 and ω_2 combine into a photon at frequency ω_3 or a photon at ω_3 splits into photons at frequencies ω_1 and ω_2.

5.4 Sum-frequency generation

Sum-frequency generation is a generalization of second-harmonic generation for two different input frequencies. In the general case, the process is governed by Eqs. (5.8)-(5.10) with the boundary condition $A_3(0) = 0$ and the other two waves applied as inputs. The general solution of these equations is again rather complicated [22].

Sum-frequency generation has a real application for the case in which the beam at frequency ω_2 can be assumed to be strong and undepleted. This process can be used to convert a weak infrared signal at frequency ω_1 to a visible frequency ω_3 by mixing with a strong intense laser beam at ω_2 [23]. This situation is described by coupled Eqs. (5.8) and (5.10) with A_2 taken as constant. For the case of perfect phase matching, the solution to the coupled equations is straightforward. For the case of no applied field at frequency ω_3, the solution is

$$A_1(z) = A_1(0)\cos\kappa z , \tag{5.14}$$

$$A_3(z) = i\left(\frac{n_1\omega_3}{n_3\omega_1}\right)^{1/2} A_1(0)\sin\kappa z e^{i\phi_2} , \tag{5.15}$$

where ϕ_2 is the phase of A_2 and the coupling constant is defined by

$$\kappa^2 = \frac{64\pi^2\omega_1\omega_3}{n_1 n_3 c^2} d^2 |A_2|^2 . \tag{5.16}$$

The energy is again seen to flow back and forth between the two fields in an oscillatory way.

5.5 *Difference-frequency generation*

We next consider the situation in which frequencies ω_3 and ω_1 are applied to the nonlinear medium to generate radiation at the difference frequency $\omega_2 = \omega_3 - \omega_1$. We assume that the field at frequency ω_3 is strong and undepleted. The propagation of the fields at frequencies ω_1 and ω_2 is then governed by Eqs. (5.8) and (5.9) with A_3 taken as constant.

For the case of perfect phase matching and boundary condition $A_2(0) = 0$, the solutions to the coupled equations are

$$A_1(z) = A_1(0)\cosh \kappa z\,, \tag{5.17}$$

$$A_2(z) = i\left(\frac{n_1\omega_2}{n_2\omega_1}\right)^{1/2} A_1^*(0)\sinh \kappa z e^{i\phi_3}\,, \tag{5.18}$$

where ϕ_3 is the phase of A_3 and the coupling constant is defined by

$$\kappa^2 = \frac{64\pi^2\omega_1\omega_2}{n_1 n_2 c^2} d^2 |A_3|^2\,. \tag{5.19}$$

Both fields are seen to grow essentially exponentially as a function of the length of the nonlinear medium. This is quite different from the case of sum-frequency generation in which the weak fields exchange energy in an oscillatory manner.

5.6 *Parametric oscillation and amplification*

The solution for the field at frequency ω_1 [Eq. (5.17)] is independent of the phase of this field. The process of difference-frequency generation is therefore seen to amplify the field at frequency ω_1. In addition, a field at frequency ω_2 is generated. The intensity of this field can grow higher than the input intensity at frequency ω_1. This process is known as parametric amplification [8,24].

The three-wave-mixing process pumped by the field at frequency ω_3 provides gain to the fields at frequencies ω_1 and ω_2. Similar to lasers, the gain can be made to oscillate by enclosing the nonlinear material in a resonator made of highly reflecting mirrors at frequency ω_1 or ω_2 (Fig. 5.3). The output frequency of such parametric oscillators can be tuned by adjusting the phase matching and the cavity resonance frequency synchronously. Parametric oscillators are presently becoming increasingly important in constructing all-solid-state sources of tunable radiation.

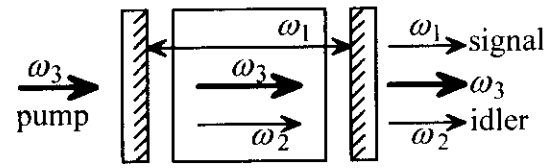

Figure 5.3. Parametric oscillator. The mirrors are highly reflecting at ω_1 and have low reflectivity at ω_2 and ω_3.

Even when the parametric gain is low and only a field at pump frequency ω_3 is applied,

there is a finite probability that a pump photon splits into two photons of lower frequency. This is equivalent to spontaneous emission in a laser gain medium. Such spontaneous parametric down-conversion (parametric fluorescence) gives rise to two photons whose properties are correlated. The correlated photons can be used to study fundamental quantum-mechanical properties of light [25].

5.7 Phase-matching

The efficiency of all the above frequency conversion processes depends on phase matching. The phase-matching condition $\Delta k = 0$ can be expressed in the form

$$n_3\omega_3 = n_1\omega_1 + n_2\omega_2 \tag{5.20}$$

In the case of no dispersion $n_3 = n_1 = n_2$, the phase matching condition would be automatically satisfied. Unfortunately, for most materials the index of refraction increases for decreasing wavelengths (Fig. 5.4). This is referred to as normal dispersion. Consequently, phase matching is one of the most important problems in second-order nonlinear optics.

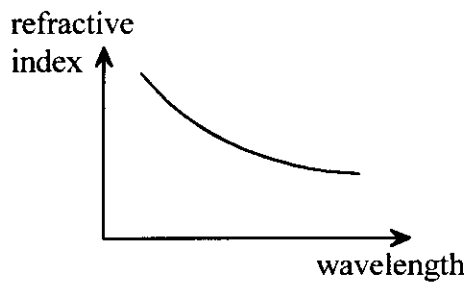

Figure 5.4. Normal dispersion.

It is possible to achieve phase matching through anomalous dispersion close to an absorption feature of a material [26]. Anomalous dispersion leads to increasing index of refraction for increasing wavelength. It can therefore be used to compensate for the effect of normal dispersion. In practice, this technique is not used, because the absorption band increases losses.

The most common way to achieve phase matching is to rely on birefringent crystals (Fig. 5.5). For example, for uniaxial crystals, the index of refraction is different for light polarized along the optic axis and perpendicular to the axis [27]. More specifically, the light polarized perpendicular to the plane containing the optic axis and the propagation vector is referred to as ordinary polarization and always experiences the ordinary index n_O. The light polarized in the plane of the axis and the propagation vector is referred to as extraordinary polarization and experiences a refractive index

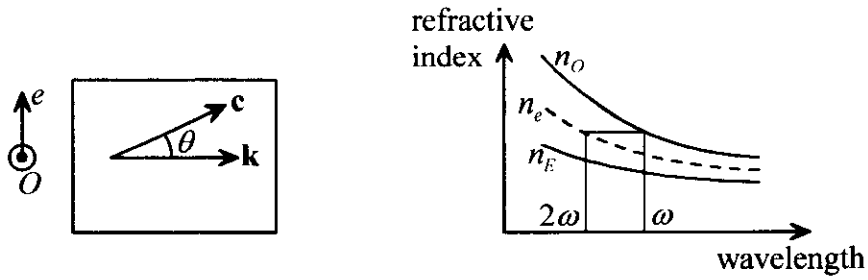

Figure 5.5. Birefringence phase matching of second-harmonic generation.

$$\frac{1}{n_e^2(\theta)} = \frac{\sin^2\theta}{n_E^2} + \frac{\cos^2\theta}{n_O^2}, \tag{5.21}$$

where θ is the angle between the axis and the propagation vector and n_E is the principal value of the extraordinary refractive index. Therefore, by changing the angle θ, phase matching can be achieved at the desired wavelength.

Phase matching is referred to as type I when the two lower frequency waves have the same polarization (ordinary or extraordinary) and type II when the polarizations are different. In general, type I phase matching is easier to achieve.

When the phase matching angle θ is different from 0 or 90 degrees, the Poynting vector **S** (energy propagation) and the propagation vector **k** (wave front propagation) point to different directions for extraordinary light. Such walkoff is a serious problem of birefringence phase matching, which limits the maximum interaction length of the process. A phase matching angle other than 90 degrees is referred to as critical. In some cases, it is possible to maintain the phase matching angle of 90 degrees and tune the phase matching wavelength by changing the temperature of the crystal. In such cases, noncritical phase matching is achieved.

Another potential problem of birefringence phase matching is that it relies on the off-diagonal components of the nonlinear susceptibility tensor. For several materials, the diagonal tensor components are largest. Diagonal (or the largest possible) tensor component can always be utilized by quasi phase matching (Fig. 5.6). Quasi phase matching is based on reversing the sign of the nonlinearity after every coherence length [22,28]. We recall that, after one coherence length, the phase relation of the converted frequency and its driving polarization is lost. However, a change in the sign of the nonlinearity reverses the sign of the driving polarization. Consequently, the phase relation between the wave and the source is restored.

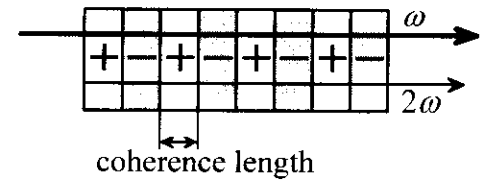

Figure 5.6. Quasi phase matching.

5.8 Linear electro-optic effect

The linear electro-optic (Pockels) effect is described by the nonlinear polarization

$$P_i(\omega) = 2\sum_{jk} \chi_{ijk}^{(2)}(\omega;\omega,0)E_j(\omega)E_k(0), \tag{5.22}$$

where **E**(0) is the (quasi)static electric field. For typical electro-optic crystals, two linear eigenpolarizations with $i = j$ are found. By taking the static field along the k direction and inserting Eq. (5.22) into the wave equation (4.4), we find

$$\nabla^2 E_i(\omega) + \frac{\omega^2}{c^2}\left[1 + 4\pi\chi_{ii}^{(1)} + 8\pi\chi_{iik}^{(2)}E_k(0)\right]E_i(\omega) = 0. \tag{5.23}$$

The linear electro-optic effect is therefore seen to change the linear index of refraction of the eigenpolarizations in the presence of the static field, i.e., the effective index is

$$n_{i,eff}^2 = (n_i + \Delta n_i)^2 = 1 + 4\pi\chi_{ii}^{(1)} + 8\pi\chi_{iik}^{(2)} E_k(0) . \tag{5.24}$$

For a small electro-optic index change, the change is

$$\Delta n_i = \frac{4\pi\chi_{iik}^{(2)} E_k(0)}{n_i} . \tag{5.25}$$

Because of the change of the refractive index, the electro-optic effect can be used for phase modulation of light.

Analogous to the other effects, we have described the electro-optic effect using the susceptibility formalism. This is not usual. Traditionally, the electro-optic effect is described in terms of the electro-optic coefficients defined as

$$\Delta\left(\frac{1}{n_i^2}\right) = r_{iik} E_k(0) . \tag{5.26}$$

From this, we obtain for small effects

$$\Delta n_i = -\frac{n_i^3 r_{iik} E_k(0)}{2} , \tag{5.27}$$

and the relation between the electro-optic coefficient and the second-order susceptibility is therefore

$$r_{iik} = -\frac{8\pi}{n_i^4}\chi_{iik} . \tag{5.28}$$

Due to the electro-optic effect, the indices of refraction of the two eigenpolarizations (x and y) become unequal. The electro-optic material therefore becomes birefringent in the presence of the static field. The material can then be used as a waveplate to control the polarization of light. The index changes of the eigenpolarizations are often equal in magnitude but opposite in sign. The phase retardation between the x and y polarizations is then

$$\phi = 2\Delta n(\omega/c)L = \frac{8\pi\omega\chi E(0)}{cn} L = -\frac{\omega n^3 r E(0)}{c} L , \tag{5.29}$$

where the notation has been simplified and L is the length of the material. Rotation of the linear polarization is obtained when the retardation between the eigenpolarizations is π. This is obtained at a voltage known as the half-wave voltage. Combination of an electro-optic polarization rotator and a linear polarizer can be used to make an intensity modulator of light.

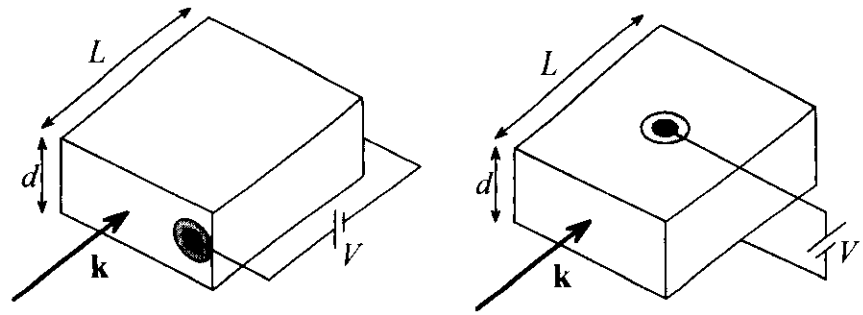

Figure 5.7. Longitudinal and transverse electro-optic configurations.

An electro-optic device can be either longitudinal or transverse (Fig. 5.7). In the longitudinal geometry, the static field is applied along the direction of propagation. The field strength is then

$$E(0) = V / L . \tag{5.30}$$

where V is the applied voltage. By Eq. (5.29), the total effect then depends only on the applied voltage and is independent of the length. The half-wave voltage of a longitudinal electro-optic device is then

$$V_{\lambda/2} = \frac{cn}{8\omega\chi} = \frac{c\pi}{\omega r n^3} . \tag{5.31}$$

In the transverse geometry, the field is

$$E(0) = V / d , \tag{5.32}$$

where d is the thickness of the device. The net effect is then proportional to the ratio L/d, and the half-wave voltage is

$$V_{\lambda/2} = \frac{d}{L}\frac{cn}{8\omega\chi} = \frac{d}{L}\frac{c\pi}{\omega r n^3} . \tag{5.33}$$

The half-wave voltage can be significantly reduced by the ratio d / L. This is particularly true in waveguided geometries.

6. Third-Order Processes

6.1 General third-order processes

The definition of the third-order nonlinear susceptibility is

$$P_i(\omega_p+\omega_q+\omega_r)=\sum_{jkl}\sum_{(pqr)}\chi^{(3)}_{ijkl}(\omega_p+\omega_q+\omega_r;\omega_p,\omega_q,\omega_r)E_j(\omega_p)E_k(\omega_q)E_l(\omega_r), \quad (6.1)$$

where the three input frequencies are, in general, different. The important difference compared to second-order processes is that no centrosymmetry rule exists for third-order processes. Hence, third-order processes are allowed in materials of all symmetry groups.

Analogous to second-order processes, third-order processes can be used for frequency conversion, for example, third-harmonic generation. Phase-matching considerations apply also to such processes and they can be treated using techniques similar to the ones used for second-order processes.

A large number of third-order processes exist that are automatically phase-matched or near-phase-matched. In the following, we will focus on such processes. In addition, we assume that all interacting fields have the same linear polarization. The scalar approximation can therefore be used. We also assume that the susceptibility is a real quantity unless specified otherwise.

6.2 Intensity-dependent refractive index

We consider the case where the optical field has only one frequency component, i.e., it can be expressed in the form

$$E(t)=E(\omega)e^{-i\omega t}+E^*(\omega)e^{i\omega t}. \quad (6.2)$$

By explicitly evaluating Eq. (6.1), we find that the third-order polarization contains a term at frequency ω given by

$$P(\omega)=3\chi^{(3)}(\omega;\omega,\omega,-\omega)\left|E(\omega)\right|^2E(\omega). \quad (6.3)$$

When the field at frequency ω consists of a single beam propagating in the positive z direction

$$E(\omega)=Ae^{ikz}, \quad (6.4)$$

we obtain a contribution

$$P(z)=3\chi^{(3)}\left|A\right|^2Ae^{ikz}, \quad (6.5)$$

which is phase-matched with the original beam. When inserted in the wave equation (4.4), we find that the influence of the third-order contribution is to change the refractive index experienced by the beam. The index is

$$n_{eff}^2 = (n + \Delta n)^2 = 1 + 4\pi\chi^{(1)} + 12\pi\chi^{(3)}|A|^2 . \tag{6.6}$$

For small nonlinear effects, the change in the index is

$$\Delta n = \frac{6\pi\chi^{(3)}|A|^2}{n} . \tag{6.7}$$

We define the nonlinear refractive index n_2 by the equation

$$n_{eff} = n + n_2 I , \tag{6.8}$$

where the intensity is

$$I = \frac{nc}{2\pi}|A|^2 . \tag{6.9}$$

By using Eqs. (6.7)-(6.9), we find that the nonlinear refractive index is

$$n_2 = \frac{12\pi^2\chi^{(3)}}{n^2 c} . \tag{6.10}$$

This process, where a strong optical beam influences the refractive index experienced by itself, is also referred to as self-phase modulation (Fig. 6.1). The change in the phase acquired in propagation is called a nonlinear phase shift.

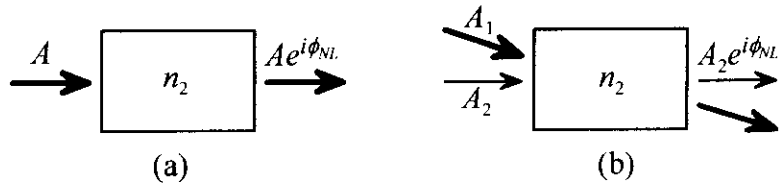

Figure 6.1. Self- (a) and cross- (b) phase modulation.

We next consider the case in which the field at frequency ω consists of a strong pump beam A_1 and a weak probe beam A_2

$$E(\omega) = A_1 e^{i\mathbf{k}_1\cdot\mathbf{r}} + A_2 e^{i\mathbf{k}_2\cdot\mathbf{r}} . \tag{6.11}$$

To first order in the weak beam A_2, the third-order nonlinear polarization contains a term

$$P = 6\chi^{(3)}|A_1|^2 A_2 e^{i\mathbf{k}_2\cdot\mathbf{r}} , \tag{6.12}$$

This term is phase matched in the direction of the weak beam. We then find that the nonlinear refractive index describing the influence of a strong beam on a weak beam is given by

$$n_2^{\text{weak}} = \frac{24\pi^2 \chi^{(3)}}{n^2 c}. \tag{6.13}$$

This process, where a strong beam influences the index experienced by a weak beam, is referred to as cross-phase modulation. The process occurs also in the case where the beams are distinguished by frequency rather than direction of propagation. Note also that the nonlinear index for cross-phase modulation is twice that for self-phase modulation. Self- and cross-phase modulations have important consequences for the propagation of short pulses in optical fibers [29].

6.3 Self-focusing and self-defocusing

Self-phase modulation makes the refractive index experienced by a beam intensity-dependent. Real laser beams often have a near Gaussian transverse profile where the highest intensity occurs in the center. For such beams, the effective index of refraction is different for different parts of the beam. Consequently, a nonlinear material can act as a lens for an intense beam.

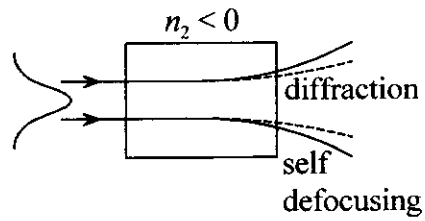

Figure 6.2. Self-defocusing.

When the nonlinear refractive index is negative, the effect is that of a negative lens. The beam then tends to diverge faster than its natural tendency due to diffraction only (Fig. 6.2). This process is called self-defocusing.

When the nonlinearity is positive, the material acts as a positive lens and tends to focus the beam (Fig. 6.3). If the nonlinear effects are small, the consequence of self-focusing is to slow the diffractive divergence of the beam. For strong nonlinear effects, self-focusing can be catastrophic and lead to optical breakdown of the material.

An interesting possibility occurs when self-focusing due to the nonlinear response is just right to counteract the effects of diffraction. In this case, the light can propagate over long distances maintaining a diameter much smaller than that allowed by diffraction. Such self-trapping occurs only when the power (not intensity) of the beam is just right (critical power) [30]. If the power is too high, the beam can break up to several filaments each containing the critical power [31].

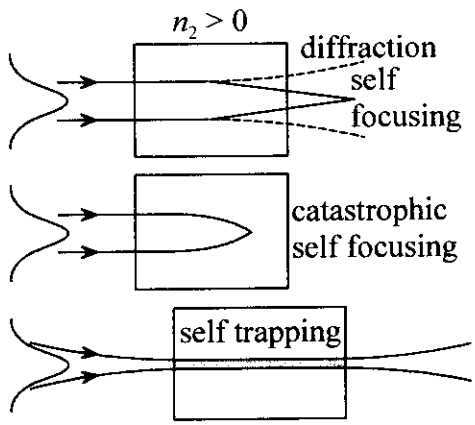

Figure 6.3. Self-focusing.

6.4 *Induced focusing*

Cross phase modulation can also lead to focusing and defocusing effects. More importantly, cross-phase modulation by a strong beam can induce focusing of a weak beam even in a material where the weak beam alone would be self defocused. The process is quite complicated, and the induced focusing is accompanied by deflection and wave breaking of the weak beam [32].

6.5 *Degenerate four-wave mixing*

Degenerate four-wave mixing is possibly the single most important third-order process. The process can occur in various different geometries. All these geometries can be described by the same basic formalism.

Degenerate four-wave mixing involves the interaction of four beams of the same frequency in a nonlinear medium. Usually two of the beams are strong pump beams and the remaining two beams are weak. The pump beams are used to control the interaction of the weak beams and to provide energy to the interaction.

We assume that the field at frequency ω can be expressed as a sum over a strong part E_p and a weak part E_w as

$$E(\omega) = E_p + E_w . \tag{6.14}$$

The nonlinear response is assumed to be due to the strong part. Hence we calculate the third-order polarization from Eq. (6.3) to first order in the weak field and obtain

$$P(\omega) = 3\chi|E_p|^2 E_p + 6\chi|E_p|^2 E_w + 3\chi E_p^2 E_w^* . \tag{6.15}$$

This result already shows that the strong part influences itself and the weak part. However, the weak part has no influence on the strong part.

To set up the equations for four-wave mixing, we express the strong field as a sum of two distinct pump beams and the weak field as a sum of two distinct beams. The strong field is therefore of the form

$$E_p = E_1 + E_2 , \tag{6.16}$$

and the weak field is of the form

$$E_w = E_3 + E_4 . \tag{6.17}$$

Note that we have not yet specified the directions of propagation of the fields. This allows us to keep the treatment of the present section as general as possible. We will only specify the directions of propagation when specific experimental geometries are considered.

By inserting Eqs. (6.16) and (6.17) into Eq. (6.15), we obtain the nonlinear polarization in the form

$$\begin{aligned} P(\omega) = {} & 3\chi|E_1|^2 E_1 + 6\chi|E_1|^2 E_2 + 3\chi E_1^2 E_2^* \\ & + 3\chi|E_2|^2 E_2 + 6\chi|E_2|^2 E_1 + 3\chi E_2^2 E_1^* \\ & + 6\chi|E_1|^2 E_3 + 6\chi|E_2|^2 E_3 + 6\chi E_1 E_2^* E_3 + 6\chi E_2 E_1^* E_3 \\ & + 6\chi|E_1|^2 E_4 + 6\chi|E_2|^2 E_4 + 6\chi E_1 E_2^* E_4 + 6\chi E_2 E_1^* E_4 \\ & + 3\chi E_1^2 E_3^* + 3\chi E_2^2 E_3^* + 6\chi E_1 E_2 E_3^* \\ & + 3\chi E_1^2 E_4^* + 3\chi E_2^2 E_4^* + 6\chi E_1 E_2 E_4^* \end{aligned} \tag{6.18}$$

This result is quite general and can be used as a starting point to treat any four-wave mixing geometry. To go further, we need to specify the harmonic spatial dependence (i.e., wave-vector dependence) of the four waves. Only terms that are phase-matched to any of the four beams are then maintained in Eq. (6.18).

6.6 Phase conjugation

As an example of the use of Eq. (6.18), we consider phase conjugation. Phase conjugation is a process where the four-wave-mixing interaction between two counter-propagating pump beams and a probe beam gives rise to a fourth beam. The fourth beam is known as the phase-conjugate of the probe beam and it propagates in a direction that is exactly opposite to the direction of propagation of the probe beam.

To define the process of phase conjugation, we express the probe beam in the form

$$\mathbf{E}_p(\omega) = \hat{\mathbf{e}}_p A_p e^{i\mathbf{k}_p \cdot \mathbf{r}}, \tag{6.19}$$

where A_p is the scalar amplitude, $\hat{\mathbf{e}}_p$ is the polarization unit vector, and the wave vector $\mathbf{k}_p$ represents the overall direction of propagation of the beam. When the plane-wave approximation is not valid, the scalar amplitude and the polarization unit vector can depend slowly on all three spatial coordinates. Analogously, we express the conjugate beam as

$$\mathbf{E}_c(\omega) = \hat{\mathbf{e}}_c A_c e^{i\mathbf{k}_c \cdot \mathbf{r}}. \tag{6.20}$$

The process of phase of phase conjugation is ideal if the following three requirements are satisfied:

1) The wave vectors of the probe and conjugate beams are opposite $\mathbf{k}_c = -\mathbf{k}_p$.

2) The scalar amplitudes of the fields are complex conjugates of each other $A_c = A_p^*$. This fact can be used to remove wave-front aberrations from an optical beam.

3) The polarization unit vectors are complex conjugates of each other $\hat{\mathbf{e}}_c = \hat{\mathbf{e}}_p^*$. This process is also known as vector phase conjugation [1]. The process can be used to remove polarization aberrations from an optical beam.

For several phase-conjugating processes, only requirements 1) and 2) are satisfied. Polarization conjugation, on the other hand, is more difficult and can be achieved only through very specific non-linear interactions [33-35].

An optical device that generates a phase-conjugate beam is known as a phase-conjugate mirror. The effect of a phase-conjugate mirror on an incident wave front is quite different from that of an ordinary mirror (Fig. 6.4). The phase-conjugate mirror reflects the light exactly back to where it came from, independent of any phase aberrations accumulated on the beam before interaction with the phase-conjugate mirror. Such aberration correction has been demonstrated in several experiments.

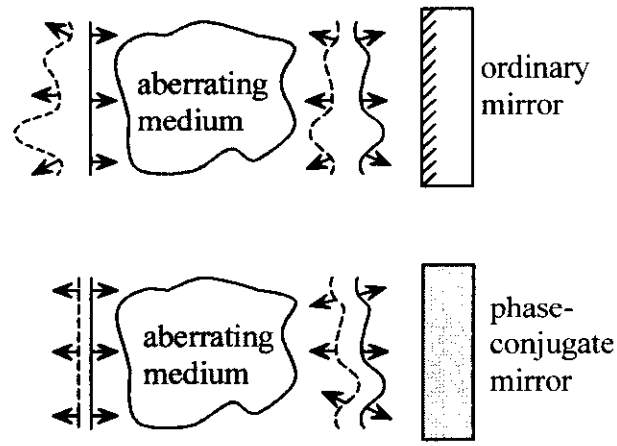

Figure 6.4. Reflection of an aberrated wave front from an ordinary and a phase-conjugate mirror.

6.7 Phase conjugation by four-wave mixing

To understand how degenerate four-wave mixing can be used to generate a phase-conjugate beam, we assume that the two strong pump beams are counter-propagating in z' direction (Fig. 6.5). We also assume that the two components of the weak field are counter-propagating in z direction. The four components of the total field are thus of the form

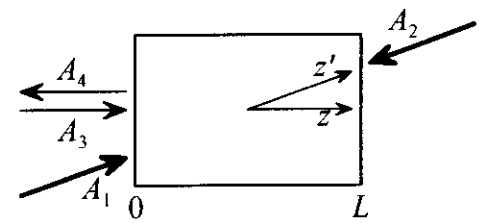

Figure 6.5. Phase conjugation by degenerate four-wave mixing.

$$E_1 = A_1 e^{ikz'}, \quad E_2 = A_2 e^{-ikz'}, \quad E_3 = A_3 e^{ikz}, \quad E_4 = A_4 e^{-ikz}, \tag{6.21}$$

where A_i are slowly-varying.

Inserting Eq. (6.21) into Eq. (6.18) and keeping only the terms that are phase-matched with any of the four beams, we find that the nonlinear polarizations driving each of the four

beams are given by

$$P_1 = (3\chi|A_1|^2 A_1 + 6\chi|A_2|^2 A_1)e^{ikz'}, \tag{6.22}$$

$$P_2 = (6\chi|A_1|^2 A_2 + 3\chi|A_2|^2 A_2)e^{-ikz'}, \tag{6.23}$$

$$P_3 = (6\chi|A_1|^2 A_3 + 6\chi|A_2|^2 A_3 + 6\chi A_1 A_2 A_4^*)e^{ikz}, \tag{6.24}$$

$$P_4 = (6\chi|A_1|^2 A_4 + 6\chi|A_2|^2 A_4 + 6\chi A_1 A_2 A_3^*)e^{-ikz}. \tag{6.25}$$

When inserted into Eq. (4.10), we find that the spatial evolution of each of the beams is governed by the equations

$$\frac{dA_1}{dz'} = i\frac{6\pi\omega}{nc}\chi(|A_1|^2 + 2|A_2|^2)A_1 = i\kappa_1 A_1, \tag{6.26}$$

$$\frac{dA_2}{dz'} = -i\frac{6\pi\omega}{nc}\chi(|A_2|^2 + 2|A_1|^2)A_2 = -i\kappa_2 A_2, \tag{6.27}$$

$$\frac{dA_3}{dz} = i\frac{12\pi\omega}{nc}\chi\left[(|A_1|^2 + |A_2|^2)A_3 + A_1 A_2 A_4^*\right], \tag{6.28}$$

$$\frac{dA_4}{dz} = -i\frac{12\pi\omega}{nc}\chi\left[(|A_1|^2 + |A_2|^2)A_4 + A_1 A_2 A_3^*\right]. \tag{6.29}$$

Note that Eqs. (6.27) and (6.29) have a different sign that Eq. (4.10). This is because beams 2 and 4 propagate in the negative z' and z directions, respectively.

Eqs. (6.26) and (6.27) describe mutual interaction of the two pump beams. This interaction is completely independent of the probe and conjugate beams. The first and second-terms on the right-hand sides of these equations represent self- and cross-phase modulation, respectively.

We assume that the third-order susceptibility is a real quantity so that neither linear nor nonlinear absorption occurs. The mutual interaction of the pump beams then only influences the phases of the beams. Eqs. (6.26) and (6.27) can then be directly solved to yield

$$A_1(z') = A_1(0)e^{i\kappa_1 z'}, \tag{6.30}$$

$$A_2(z') = A_2(0)e^{-i\kappa_2 z'}. \tag{6.31}$$

Eqs. (6.28) and (6.29) contain terms that describe cross-phase modulation by the pump beams and terms that describe coupling of the probe and phase-conjugate fields through the four-wave mixing interaction. Note that this coupling depends on the quantity

$$A_1(z')A_2(z') = A_1(0)A_2(0)e^{i(\kappa_1 - \kappa_2)z'}. \tag{6.32}$$

This result implies that the phase-matching condition of the four-wave-mixing process is

modified by the nonlinear phase shift of the pump waves due to their mutual interaction. Only for the case of equal pump-wave amplitudes is the phase-matching condition preserved.

For simplicity, we assume that the pump beams have equal amplitudes. We also assume that the pump beams are not depleted by the four-wave-mixing interaction. The mutual coupling of the probe and conjugate beams is then represented by the equations

$$\frac{dA_3}{dz} = i\kappa_3 A_3 + i\kappa A_4^*, \tag{6.33}$$

$$\frac{dA_4}{dz} = -i\kappa_3 A_4 - i\kappa A_3^*, \tag{6.34}$$

where the coupling constants are

$$\kappa_3 = \frac{12\pi\omega}{nc}\chi(|A_1|^2 + |A_2|^2), \tag{6.35}$$

$$\kappa = \frac{12\pi\omega}{nc}\chi A_1 A_2. \tag{6.36}$$

The solution to these equations is straightforward. For the case of no phase-conjugate input at $z = L$, the transmitted probe beam is found to be

$$A_3(L) = e^{i\kappa_3 L}\frac{A_3(0)}{\cos\kappa L}, \tag{6.37}$$

and the reflected conjugate beam is

$$A_4(0) = iA_3^*(0)\tan\kappa L. \tag{6.38}$$

These solutions show that the four-wave-mixing process can amplify the probe beam and simultaneously generate a phase conjugate beam with higher intensity than that of the initial probe beam. Such amplification occurs at the expense of the pump beams. One possible photon diagram describing this is shown in Fig. 6.6. Note that the situation is very similar to that of parametric down conversion by difference-frequency generation (Sections 5.5 and 5.6).

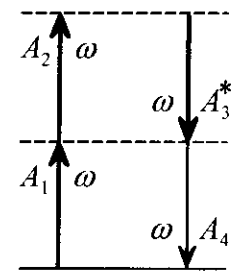

Figure 6.6. An example of a photon diagram describing degenerate four-wave mixing.

7. Nonlinear Optical Materials

7.1 Requirements for nonlinear materials

The principal requirement for a good nonlinear material is a high value of the nonlinear response. However, a number of other properties are also required from useful materials. The material should have low loss at the operation wavelengths. To minimize absorption losses, the operation wavelengths must be sufficiently longer than the principal absorption band of the material. In practice, this condition prevents the use of strongly resonantly-enhanced nonlinearities in applications. To minimize the scattering losses, the optical quality of the material should be high.

For several applications, the nonlinear response should be very fast. For such applications, one should consider materials where the nonlinearity has an electronic origin. Response times in the femtosecond regime can then be expected.

The nonlinear materials should also be easy to process into device configurations, such as wave-guides, and the nonlinear response should be stable under the operating conditions. Long-term thermal stability at temperatures of 80-100 °C is important for several potential applications. In addition, for widespread applications, the materials should be inexpensive.

Second-order nonlinear materials have additional requirements, most importantly, the requirement of noncentrosymmetry. For frequency conversion, a method to phase match the interaction is needed. In addition, the speed of electro-optic devices is limited by the capacitance of the device. For low capacitance, materials with small low-frequency dielectric constant are desirable.

7.2 Organic materials

Organic molecular materials have been recognized as one of the most promising groups of nonlinear materials. The properties of such materials can be easily modified through chemical synthesis to optimize their nonlinear response and other properties. In addition, they are potentially inexpensive and can be easily processed into various device configurations such as thin-film wave guides. Compared to inorganic crystals ($\varepsilon >$ 5-10), organic materials have a low dielectric constant (~3), which is beneficial for electro-optic applications.

In the following, we will discuss some very basic issues that are related to the development and characterization of organic nonlinear materials. In addition, we will describe some new approaches that could become useful in materials development to overcome some of the existing problems in organic nonlinear optics. We will focus on second-order nonlinear materials, because the design rules for good second-order materials are quite well defined. On the other hand, all materials have a third-order response and no well-defined rules exist for the optimization of third-order materials. It is also possible that through cascading effects [36], second-order materials can be used for certain third-order applications.

7.3 Microscopic response

The basic building unit for organic nonlinear materials is a nonlinear molecule or chromophore. For second-order nonlinear optics, noncentrosymmetric chromophores with a nonvanishing first hyperpolarizability β are required.

Traditional second-order nonlinear chromophores contain an electron donating group (donor) and electron accepting group (acceptor) that are connected by a conjugated π electron system (Fig. 7.1). The π electrons [37] are delocalized over the conjugated system and are thus easily polarizable. The donor and acceptor groups break the centrosymmetry and the charge distribution of the molecule is asymmetric with excess charge at the acceptor. Consequently, the molecule has a permanent dipole moment.

The conjugated second-order molecules can often be assumed to be almost one-dimensional. In such cases, the molecular hyperpolarizability has only one dominant component β_{ZZZ}, where Z is the axis connecting the donor and acceptor groups.

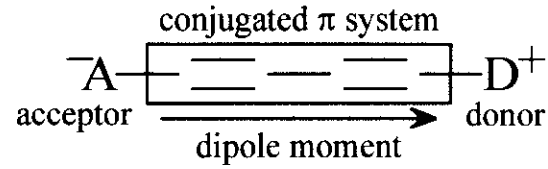

Figure 7.1. A typical second-order nonlinear molecule.

7.4 Electric-field-induced second-harmonic generation (EFISHG)

The nonlinear properties of molecules are most convenient to measure by dissolving the molecules in an appropriate solvent. In the solution, the molecules are randomly oriented (isotropic) and the microscopic nonlinear response of the individual molecules usually averages to zero on the macroscopic level. Consequently, an isotropic solution has no macroscopic second-order response.

The macroscopic centrosymmetry of the solution can be broken by applying a static electric field over the sample. It then becomes possible to use the solution for second-harmonic generation (Fig. 7.2). This process is known as electric-field-induced second-harmonic generation (EFISHG).

The nonlinear response of EFISHG has two distinct contributions. The first contribution is due to the second hyperpolarizability (third-order nonlinearity)

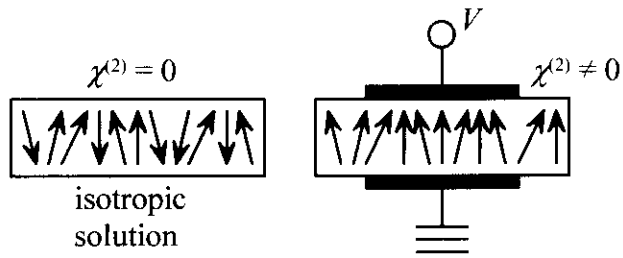

Figure 7.2. Alignment of molecular dipoles by a static electric field for EFISHG.

$$\mu(2\omega) = \gamma(2\omega;\omega,\omega,0)E^2(\omega)E_0, \tag{7.1}$$

where E_0 is the static field. The second contribution is due to the interaction of the permanent dipole moments of the molecules with the static field, which tends to align the molecules parallel to the field. The interaction energy between the dipole μ_0 and the static field is $H = -\mu_0 \cdot \mathbf{E}_0$. The degree of orientation achieved depends also on the thermal energy kT. The result is that, for low values of the static field, the macroscopic nonlinear polarization at the second harmonic frequency is

$$P(2\omega) = \chi^{(3)}_{eff}(2\omega;\omega,\omega,0)E^2(\omega)E_0 = \chi^{(2)}_{eff}(2\omega;\omega,\omega)E^2(\omega), \tag{7.2}$$

where the effective susceptibilities are is

$$\chi^{(3)}_{eff}(2\omega;\omega,\omega,0) = NF\left[\langle\gamma(2\omega;\omega,\omega,0)\rangle + \frac{\mu_0 \cdot \beta_{vec}(2\omega;\omega,\omega)}{5kT}\right], \tag{7.3}$$

$$\chi^{(2)}_{eff}(2\omega;\omega,\omega) = \chi^{(3)}_{eff}(2\omega;\omega,\omega,0)E_0. \tag{7.4}$$

Here β_{vec} is the vectorial part of the first hyperpolarizability, $\langle\gamma(2\omega;\omega,\omega,0)\rangle$ is the isotropically averaged second hyperpolarizability, F is the total local field factor, and N is the number density of the dissolved molecules.

These results are only valid for sufficiently low static fields that no saturation of the molecular alignment occurs [4]. For good second-order materials, the part due to the first hyperpolarizability β dominates the nonlinear response. Note also that the net nonlinear response is due to the product of the permanent dipole moment and the first hyperpolarizability. The method can be used to determine the value of the hyperpolarizability only if some other method is used to determine the value of the dipole moment [38].

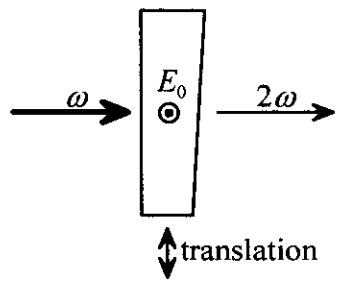

Figure 7.3. A typical wedged EFISHG cell.

Second-harmonic generation in an EFISHG-experiment is not phase-matched. Consequently, the experiments are done using a cell with two windows that are not parallel (Fig. 7.3). The cell is translated to vary the pathlength and to record the sinusoidal variation of the second-harmonic signal (Eq. 4.19) as a function of the pathlength.

7.5 Hyper-Rayleigh scattering (HRS)

EFISHG is only applicable to molecules with a permanent dipole moment. However, there are also second-order nonlinear molecules with a vanishing dipole moment. The second-order nonlinear properties of such octopolar systems [39] can not be determined by EFISHG. In addition, EFISHG is not applicable to ionic materials.

Hyper-Rayleigh scattering is a technique that can be used to determine the first hyperpolarizability of any material in solution [40-42]. The technique is based on the fact that, in isotropic solutions, each molecule still has a microscopic nonlinear response, although the solution is macroscopically centrosymmetric. The macroscopic centrosymmetry only excludes coherent second-order processes. Nevertheless, each molecular dipole still emits its characteristic radiation pattern. In the case that the molecules are not orientationally correlated, the molecular radiation patterns add incoherently in any direction. This incoherent radiation is hyper-Rayleigh scattering.

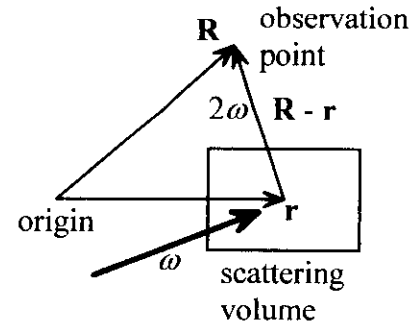

Figure 7.4. Geometry to analyze hyper-Rayleigh scattering.

To analyze Hyper-Rayleigh scattering (Fig. 7.4), we express the fundamental field components as

$$E_i(\omega) = A_i e^{i\mathbf{k}\cdot\mathbf{r}}. \tag{7.5}$$

At location $\mathbf{r}$, the i component of the molecular dipole moment at the second-harmonic frequency is then

$$\mu_i = \beta_{ikl}(\mathbf{r}) A_k A_l e^{i2\mathbf{k}\cdot\mathbf{r}}, \tag{7.6}$$

where summation over repeated indices kl is implied. Note that the hyperpolarizability has spatial dependence, because it is now defined in the laboratory frame and is therefore different for each molecule. The second-harmonic field at the observation point $\mathbf{R}$ is then obtained as a sum over fieldlets emitted by all molecules in the scattering volume

$$E_i(2\omega) = \sum_u g(\mathbf{r}_u)\mu_i(\mathbf{r}_u) e^{iK|\mathbf{R}-\mathbf{r}_u|}, \tag{7.7}$$

where $g(\mathbf{r}_u)$ represents the radiation efficiency from the location of the molecule $\mathbf{r}_u$ to the observation point, and K is the magnitude of the wave vector at the second-harmonic frequency. The intensity of the second-harmonic field depends on the cross correlation function

$$\begin{aligned} I_{ij}(2\omega) &= E_i(2\omega)E_j^*(2\omega) \\ &= \sum_u |g(\mathbf{r}_u)|^2 \mu_i(\mathbf{r}_u)\mu_j^*(\mathbf{r}_u) \\ &\quad + \sum_{u\neq v} g(\mathbf{r}_u)g^*(\mathbf{r}_v)\mu_i(\mathbf{r}_u)\mu_j^*(\mathbf{r}_v) e^{iK|\mathbf{R}-\mathbf{r}_u|} e^{-iK|\mathbf{R}-\mathbf{r}_v|}. \end{aligned} \tag{7.8}$$

The second term of Eq. (7.8) represents coherent second-harmonic generation. For the case in which the individual molecules have no orientational correlation, this contribution vanishes.

The first term of Eq. (7.8) on the other hand depends only on the properties of individual molecules and gives rise to the incoherent radiation at the second-harmonic frequency, i.e., to the hyper-Rayleigh scattering signal.

The incoherent part is

$$I_{ij}(2\omega) = \sum_u |g(\mathbf{r}_u)|^2 \beta_{ikl}(\mathbf{r}_u)\beta^*_{jmn}(\mathbf{r}_u) A_k A_l A^*_m A^*_n$$
$$= GN\left\langle \beta_{ikl}\beta^*_{jmn}\right\rangle A_k A_l A^*_m A^*_n , \qquad (7.9)$$

where N is the number density of the molecules, the angular brackets represent averaging over the orientational distribution function of a single molecule, and G is an overall factor of proportionality. The hyper-Rayleigh scattering signal therefore depends on the orientational average of the quadratic combination of the components of the first hyperpolarizability tensor. This quantity can be transformed into the molecular frame to analyze the properties of the molecular tensor.

In addition to hyper-Rayleigh scattering at the second-harmonic frequency, more general second-order light scattering with two different input frequencies has been observed [43]. In both cases, polarization techniques can be used to increase the amount of information on the molecular hyperpolarizability tensor [43,44]. Unfortunately, the full tensor analysis of second-order light scattering is very complicated [45].

7.6 Macroscopic response

For a macroscopic device configuration, the nonlinear molecules must be organized in a noncentrosymmetric way. The most common way of doing this is by poling (Fig. 7.5). The chromophores are first incorporated in a polymer matrix. The polymer is then spin coated on a substrate to form a thin-film structure. After spin coating, the chromophores have isotropic orientational distribution and the system has no second-order nonlinearity.

To break the centrosymmetry, the polymer is heated close to its glass-transition temperature T_g, which increases the mobility of the chromophores. The chromophores are then aligned by the application of a static electric field as in EFISHG. In the end, the alignment is frozen-in by cooling the sample below the glass-transition temperature while the static field is on. Such poled polymer films can be

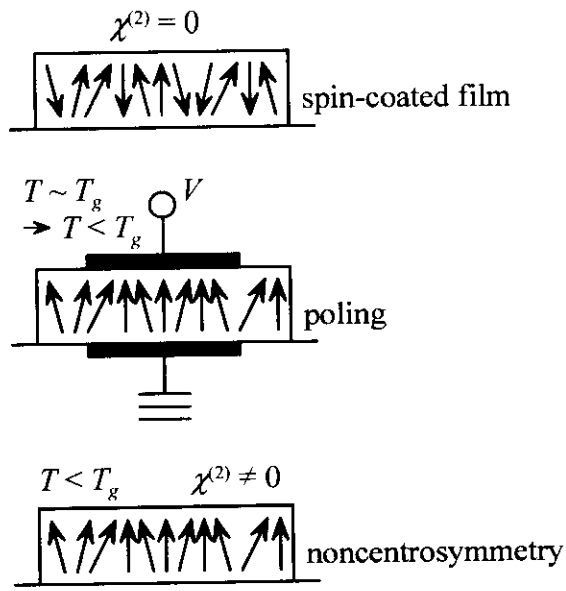

Figure 7.5. Poling of nonlinear chromophores in an electric field.

used to make wave-guided second-order devices.

The main problem with poled systems is that they are thermodynamically unstable. Hence, the ordering of the chromophores tends to relax with time, which leads to a decrease in the nonlinear response. Traditionally, this has been the most important problem of poled systems. However, recent work has demonstrated significant improvements in the stability of poled materials [46].

7.7 Orientational correlation of chromophores

One way of improving the performance of poled materials is to use rigid molecular structures with several orientationally correlated chromophores [47,48]. The permanent dipole moment and the first hyperpolarizability of the mesoscopic (supramolecular) structure are then obtained as coherent superpositions of the respective molecular quantities.

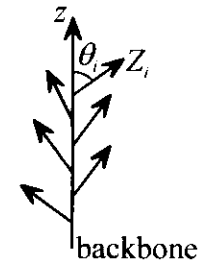

Figure 7.6. Orientationally correlated chromophores attached on a backbone.

As an example, we consider the system of Fig. 7.6, where the chromophores have a net alignment along the z (mesoscopic frame) direction but the transverse orientation is random. We also assume that the hyperpolarizability of the chromophores has a dominant $\beta_{ZZZ} = \beta_0$ (chromophoric frame) component and that their dipole moment is also along the Z direction.

The dipole moment of the mesoscopic structure is then given by

$$\mu = n\mu_0\langle\cos\theta\rangle, \tag{7.10}$$

where μ_0 is the dipole moment of a single chromophore, θ is the angle between the mesoscopic and chromophoric axes, n is the number of orientationally correlated chromophores, and the brackets denote averaging over the orientational distribution of the chromophores. Similarly, the vectorial part of the mesoscopic hyperpolarizability is given by

$$\beta = n\beta_0\langle\cos\theta\rangle. \tag{7.11}$$

We recall that the macroscopic nonlinearity of poled materials depends on the product $\mu\beta$ (Eq. 7.3). In the mesoscopic structure, this product per chromophore is

$$\frac{\mu\beta}{n} = n\mu_0\beta_0\langle\cos\theta\rangle^2. \tag{7.12}$$

This quantity is seen to be enhanced compared to individual chromophores whenever [47,48]

$$n\langle\cos\theta\rangle^2 > 1. \tag{7.13}$$

Further enhancement of the product $\mu\beta$ can be obtained from the dipole moment of the backbone of the mesoscopic structure [49]. These principles have been utilized to enhance the product $\mu\beta$ by a factor of 35 indicating a potential 1000-fold increase in the efficiency $[\sim(\mu\beta)^2]$ of the nonlinear response of poled materials [47]. In practice, the enhancement factor will most likely to be lower, because a large value of the dipole moment leads to saturation (near-perfect alignment of the chromophores) in the poling process.

7.8 Chiral materials

Chiral molecules have no reflection symmetry and occur in two different enantiomers that are mirror images of each other (Fig. 7.7). In linear optics, such molecules are known for their optical activity, e.g., rotation of the plane of polarization as linearly polarized light traverses the chiral medium [9,50]. Optical activity effects arise from the different interaction of chiral media with left- and right-hand circularly-polarized light. In isotropic materials, optical activity is due to contributions of magnetic-dipole transitions to the linear optical properties of chiral media.

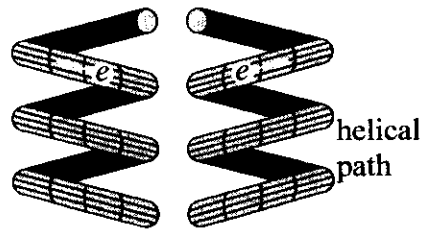

Figure 7.7. Left- and right-handed enantiomers of a helical model of a chiral molecule.

Chiral materials have interesting second-order nonlinear properties. Due to the low molecular symmetry, highly symmetric macroscopic samples (e.g., isotropic solutions) of a single enantiomer are noncentrosymmetric with a nonvanishing second-order response [51,52]. Chirality can also be used to ensure that a material crystallizes in a noncentrosymmetric way [53].

The components of the second-order susceptibility tensor of a chiral material can be classified as achiral (allowed for a racemic 50/50 mixture of the enantiomers) or chiral (allowed only for a chiral sample). For example, in an isotropic solution, the tensor component χ_{xyz} is chiral. This tensor component reverses its sign under reflection in plane and must therefore vanish in a racemic sample with reflection symmetry.

In our group, we have recently investigated second-order nonlinear properties of thin films of a chiral helicene molecule [54]. In the films, the molecule forms aggregates with chiral properties enhanced over those of the individual molecules. For the case of nonracemic (only one enantiomer) films, a very high second-order nonlinear response was observed. On the other hand, the nonlinear response of a racemic sample was a factor of 1000 lower. This is particularly interesting, because the helicene itself is not optimized for second-order nonlinear optics. The high nonlinearity was shown to arise from the chirality of the nonracemic sample.

Chiral molecules can also have strong magnetic-dipole transitions. Symmetry properties of magnetic-dipole transitions are different from those of electric-dipole transitions (see Section 8). Second-order nonlinear processes involving magnetic (or quadrupole) transitions can therefore be allowed also in centrosymmetric materials [55].

8. Higher-Multipole Nonlinearities

8.1 Hamiltonian

The interaction energy between the electromagnetic field and the material can be expanded in the multipole form [2,6,56]

$$H = -\boldsymbol{\mu}\cdot\mathbf{E} - \mathbf{m}\cdot\mathbf{B} - \mathbf{Q}\cdot\nabla\mathbf{E}, \tag{8.1}$$

where $\mathbf{E}$ is the electric field, $\mathbf{B}$ is the magnetic induction field, $\boldsymbol{\mu}$ is the electric dipole moment, $\mathbf{m}$ is the magnetic dipole moment, and $\mathbf{Q}$ is the electric quadrupole moment of the material.

The first term of Eq. (8.1) describes the electric-dipole interaction. This is usually the leading contribution. Up to this point, we have only considered nonlinearities that arise from the electric-dipole interaction. For example, the quantum-mechanical expression for the first hyperpolarizability (Eq. 3.15) only includes electric-dipole transition moments.

8.2 Susceptibilities

In most materials, the electric-dipole interaction is expected to be stronger than the magnetic-dipole and electric-quadrupole interactions [57]. To go beyond electric-dipole approximation, it is therefore sufficient to treat the magnetic and quadrupole interactions to first order [58,59]. This allows us to define four new susceptibility tensors that account for the higher multipole interactions. As an example, we consider second-harmonic generation.

Up to first order in the magnetic and quadrupole interactions, the nonlinear polarization at the second-harmonic frequency is

$$\begin{aligned} P_i(2\omega) = {} & \chi_{ijk}^{eee}(2\omega,\omega,\omega)E_j(\omega)E_k(\omega) + \chi_{ijk}^{eem}(2\omega,\omega,\omega)E_j(\omega)B_k(\omega) \\ & + \chi_{ijkl}^{eeQ}(2\omega,\omega,\omega)E_j(\omega)\nabla_k E_l(\omega). \end{aligned} \tag{8.2}$$

In addition, the material develops a nonlinear magnetization

$$M_i(2\omega) = \chi_{ijk}^{mee}(2\omega,\omega,\omega)E_j(\omega)E_k(\omega), \tag{8.3}$$

and quadrupolarization

$$Q_{ij}(2\omega) = \chi_{ijkl}^{Qee}(2\omega,\omega,\omega)E_k(\omega)E_l(\omega). \tag{8.4}$$

In Eqs. (8.2)-(8.4), the superscripts associate the respective subscripts with the electric-dipole (e), magnetic-dipole (m), and electric quadrupole (Q, two subscripts) interactions. For example, for the case of tensor χ^{eem}, the magnetic interaction is associated with annihilation of one of the fundamental photons, whereas for the case of χ^{mee}, the magnetic interaction is associated with the creation of the second-harmonic photon (Fig. 8.1).

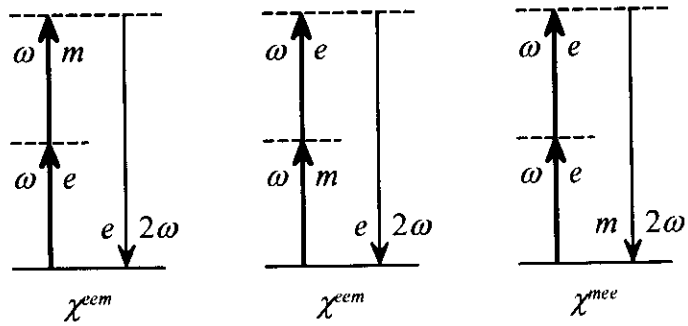

Figure 8.1. Photon diagrams describing the magnetic susceptibility tensors and indicating the multipole interactions.

The quantum-mechanical expressions for the higher multipole tensors are similar to Eq. (3.15) with one of the electric-dipole moments replaced by a magnetic-dipole or electric-quadrupole moment.

8.3 Effective polarization

The effect of the polarization, magnetization, and quadrupolarization sources is often expressed in terms of the effective polarization

$$\mathbf{P}_{eff}(2\omega) = \mathbf{P}(2\omega) + i\frac{c}{2\omega}\nabla\times\mathbf{M}(2\omega) + \nabla\cdot\mathbf{Q}(2\omega)\,. \tag{8.5}$$

However, this expression is valid only for coherent radiation in the forward direction. Great care must be exercised in the case of thin film nonlinear optics to account for the different radiative properties of the multipole sources in the forward and backward directions [60,61].

8.4 Symmetry properties

The important difference between the electric-dipole tensor χ^{eee} and the higher multipole tensors is their symmetry properties. These differences are a direct consequence of the different character of electric and magnetic quantities.

Electric quantities are polar vectors [50] that transform as the position vector under various spatial symmetry operations. The magnetic quantities, on the other hand, are axial vectors that transform as the position vector under proper transformations (rotations) only. Under improper transformations (reflection, inversion), each component of an axial vector transforms opposite to that of the position vector.

For the case of a centrosymmetric material, inversion is a symmetry operation. The various quantities then transform as

$$\mathbf{r}\to-\mathbf{r},\ \mathbf{E}\to-\mathbf{E},\ \mathbf{P}\to-\mathbf{P},\ \mathbf{B}\to\mathbf{B},\ \mathbf{M}\to\mathbf{M}\,. \tag{8.6}$$

We then find that

$$-\mathbf{P} = \chi^{eem} : (-\mathbf{E})(\mathbf{B}) = -\chi^{eem} : \mathbf{EB} = -\mathbf{P}, \tag{8.7}$$

which implies that χ^{eem} is nonvanishing in centrosymmetric materials. By similar arguments, χ^{mee} is also nonvanishing. In addition, χ^{eeQ} and χ^{Qee} are third-rank tensors that depend only on polar quantities. They are therefore allowed in all materials including centrosymmetric ones.

8.5 Materials with higher multipole nonlinearities

Electric-dipole interactions are usually much stronger than the higher multipole interactions. However, the second-order nonlinear response may be electric-dipole-forbidden for symmetry reasons. The higher multipole interactions are expected to become important in such occasions [62].

Electric-quadrupole nonlinearities can also be important in nonlinear optics of surfaces and interfaces [63]. At the boundary of two media, the normal component of the electric field experiences a discontinuity. Consequently, the gradient $\nabla\mathbf{E}$ can be very high favoring the quadrupole interaction.

In some case, the structure of the material can be expected to favor higher multipole contributions. For example, the importance of magnetic interactions in chiral media is well-established [50]. The second-order nonlinear response of centrosymmetric crystals consisting of the two enantiomers of a chiral molecule has been explained by a magnetic nonlinearity [55]. In addition, the magnetic contributions (including possibly some quadrupole contributions) have been shown to be comparable to the electric contributions in the nonlinear response of thin films of chiral molecules [64].

References

1. R. W. Boyd, *Nonlinear Optics* (Academic, San Diego, 1992).
2. Y. R. Shen, *The Principles of Nonlinear Optics* (Wiley, New York, 1984).
3. P. N. Butcher and D. Cotter, *The Elements of Nonlinear Optics* (Cambridge, Cambridge, 1990).
4. P. N. Prasad and D. J. Williams, *Introduction to Nonlinear Optical Effects in Molecules and Polymers* (Wiley, New York, 1991).
5. Ch. Bosshard, K. Sutter, Ph. Pretre, J. Hullinger, M. Flörsheimer, P. Kaatz, and P. Günter, *Organic Nonlinear Optical Materials* (Gordon and Breach, Basel, 1995).
6. N. Bloembergen, *Nonlinear Optics, Fourth Printing* (Benjamin, Reading, 1982).
7. H. Rabin and C. L. Tang, editors, *Quantum Electronics, Volume I, Parts A and B* (Academic, New York, 1975).
8. A. Yariv, *Quantum Electronics, Third Edition* (Wiley, New York, 1989).
9. G. H. Wagniere, *Linear and Nonlinear Optical Properties of Molecules* (VCH, Weinheim, 1993).
10. D. S. Chemla and J. Zyss, editors, *Nonlinear Optical Properties of Organic Molecules and Crystals, Volumes 1 and 2* (Academic, Orlando, 1987).
11. R. A. Fisher, editor, *Optical Phase Conjugation* (Academic, Orlando, 1983).
12. J. E. Sipe and R. W. Boyd, Phys. Rev. A **46**, 1614 (1992).
13. G. L. Fischer, R. W. Boyd, R. J. Gehr, S. A. Jenekhe, J. A. Osaheni, J. E. Sipe, and L. A. Weller-Brophy, Phys. Rev. Lett. **74**, 1871 (1995).
14. R. J. Gehr, G. L. Fischer, R. W. Boyd, and J. E. Sipe, Phys. Rev. A **53**, 2792 (1996).
15. N. Bloembergen, H. Lotem, and R. T. Lynch, Jr., Indian J. Appl. Phys. **16**, 151 (1978).
16. N. W. Ashcroft and N. D. Mermin, *Solid State Physics* (Holt-Rinehart-Winston, New York, 1976).
17. J. D. Donaldson and S. D. Ross, *Symmetry and Stereochemistry* (Intertext, London, 1972).
18. W. K. H. Panofsky and M. Phillips, *Classical Electricity and Magnetism* (Addison-Wesley, Reading, 1978).
19. D. L. Andrews, in *Modern Nonlinear Optics, Part 2*, edited by M. Evans and S. Kielich (Wiley, New York, 1993).
20. N. Bloembergen and P. S. Pershan, Phys. Rev. **128**, 606 (1962).
21. J. E. Sipe, J. Opt. Soc. Am. **4**, 481 (1987).
22. J. A. Armstrong, N. Bloembergen, J. Ducuing, and P. S. Pershan, Phys. Rev. **127**, 1918 (1962).
23. R. W. Boyd and C. H. Townes, Appl. Phys. Lett. **31**, 440 (1977).
24. R. L. Byer, in *Quantum Electronics, Volume I, Part B*, edited by H. Rabin and C. L. Tang (Academic, New York, 1975).

25. L. Mandel and E. Wolf, *Optical Coherence and Quantum Optics* (Cambridge, Cambridge, 1995).
26. P. A. Cahill, K. D. Singer, and L. A. King, Opt. Lett. **14**, 1137 (1989).
27. M. Born and E. Wolf, *Principles of Optics, Sixth Edition* (Pergamon, Oxford, 1980).
28. M. M. Fejer, G. A. Magel, D. H. Jundt, and R. L. Byer, IEEE J. Quantum Electron. **28**, 2631 (1992).
29. G. P. Agrawal, *Nonlinear Fiber Optics* (Academic, San Diego, 1989).
30. J. E. Bjorkholm and A. Ashkin, Phys. Rev. Lett. **32**, 129 (1974).
31. V. Bespalov and V. I. Talanov, JETP Lett. **3**, 471 (1966).
32. A. J. Stentz, M. Kauranen, J. J. Maki, G. P. Agrawal, and R. W. Boyd, Opt. Lett. **17**, 19 (1992).
33. E. J. Miller and R. W. Boyd, Opt. Lett. **15**, 1188 (1990).
34. W. R. Tompkin, M. S. Malcuit, and R. W. Boyd, J. Opt. Soc. Am. B **6**, 757 (1989).
35. M. Kauranen and R. W. Boyd, Phys. Rev. A **44**, 584 (1991).
36. G. Stegeman, R. Schiek, L. Torner, W. Torruellas, Y. Baek, D. Baboui, Z. Wang, E. Van Stryland, D. Hagan, and G. Assanto, in *Novel Optical Materials and Applications*, edited by I.-C. Khoo, F. Simoni, and C. Umeton (Wiley, New York, 1997).
37. K. P. C. Vollhardt and N. E. Schore, *Organic Chemistry, Second Edition* (Freeman, New York, 1994).
38. B. K. P. Scaife, *Principles of Dielectrics* (Clarendon, Oxford, 1989).
39. J. Zyss, Nonlinear Opt. **1**, 3 (1991).
40. R. W. Terhune, P. D. Maker, C. M. Savage, Phys. Rev. Lett. **14**, 681 (1965).
41. K. Clays and A. Persoons, Phys. Rev. Lett. **66**, 2980 (1991).
42. K. Clays and A. Persoons, Rev. Sci. Instrum. **63**, 3285 (1992).
43. T. Verbiest, M. Kauranen, and A. Persoons, J. Chem. Phys. **101**, 1745 (1994).
44. G. J. T. Heesink, A. G. T. Ruiter, N. F. van Hulst, and B. Bölger, Phys. Rev. Lett. **71**, 999 (1993).
45. M. Kauranen and A. Persoons, J. Chem. Phys. **104**, 3445 (1996).
46. T. Verbiest, D. M. Burland, M. C. Jurich, V. Y. Lee, R. D. Miller, and W. Volksen, Science **268**, 1604 (1995).
47. M. Kauranen, T. Verbiest, C. Boutton, M. N. Teerenstra, K. Clays, A. J. Schouten, R. J. M. Nolte, and A. Persoons, Science **270**, 966 (1995).
48. T. Verbiest, C. Samyn, C. Boutton, C. Houbrechts, M. Kauranen, and A. Persoons, Adv. Mater. **8**, 756 (1995).
49. B. F. Levine and C. G. Bethea, J. Chem. Phys. **63**, 2666 (1975).
50. L. Barron, *Molecular Light Scattering and Optical Activity* (Cambridge, Cambridge, 1982).
51. P. M. Rentzepis, J. A. Giordmaine, and K. W. Wecht, Phys. Rev. Lett. **16**, 792 (1966).
52. A. P. Shkurinov, A. V. Dubrovskii, and N. I. Koroteev, Phys. Rev. Lett. **70**, 1085 (1993).

53. J. Zyss and D. S. Chemla, in *Nonlinear Optical Properties of Organic Molecules and Crystals, Volume 1*, edited by D. S. Chemla and J. Zyss (Academic, Orlando, 1987).
54. C. Nuckolls, T. J. Katz, and L. Castellanos, J. Am. Chem. Soc. **118**, 3767 (1996).
55. E. W. Meijer, E. E. Havinga, and G. L. J. A. Rikken, Phys. Rev. Lett. **65**, 37 (1990).
56. J. Fiutak, Can. J. Phys. **41**, 12 (1963).
57. R. Loudon, *The Quantum Theory of Light, Second Edition* (Oxford, Oxford, 1983).
58. P. S. Pershan, Phys. Rev. **130**, 919 (1963).
59. E. Adler, Phys. Rev. **134**, A728 (1964).
60. J. De Goede and P. Mazur, Physica **58**, 568 (1972).
61. J. J. Maki, M. Kauranen, and A. Persoons, Phys. Rev. B **51**, 1425 (1995).
62. R. W. Terhune, P. D. Maker, C. M. Savage, Phys. Rev. Lett. **8**, 404 (1962).
63. P. Guyot-Sionnest and Y. R. Shen, Phys. Rev. B **35**, 4420 (1987).
64. M. Kauranen, J. J. Maki, T. Verbiest, S. Van Elshocht, and A. Persoons, Phys. Rev. B **55**, R1985 (1997).